POLITECNICO DI TORINO

Master's Degree in Communications Engineering

Master's Degree Thesis

Simulation and Modeling Optical Transmission in Dispersion Managed Scenarios

Supervisors

Prof. Emanuele VIRGILLITO

Prof. Vittorio CURRI

Candidate

Rosario IETRO

April 2025

Summary

In recent years, optical fibers became increasingly important means for huge amount of data transport. As time goes on, data dimensions requested become higher and higher, and deployment of submarine links based on optical fibers cables has spread out in all the world. Most recent systems use coherent technology in order to satisfy such data requests due to the fact that coherent transceiver exploits power, phase and polarization modulation. But there exist submarine cables deployed in the past that used to work with older, IMDD (Intensity-Modulation Direct-Detection) technology, in which only power modulation was used to carry information. The peculiarity of these links is that chromatic dispersion is compensated periodically along the fiber spans (Dispersion Managed, DM), by placing Dispersion Compensation Units (DCU). These dispersion compensation maps were engineered ad-hoc to tradeoff between inter-symbol interference compensation and mitigation of non-linearities. Instead, coherent transmission does not need inline chromatic dispersion compensation periodically but dispersion is accumulated and compensated through DSP at the receiver (Uncompensated Transmission, UT) as their nonlinearity is severely impaired by small inline redisual dispersion due to the coherent accumulation between the noise contribution introduced by each fiber span. However, today companies want to still exploit such submarine DM cables leaved from IMDD legacy, since substitution of them in favor of coherent-suited transceiver would be very impactful from an economic point of view. In order to satisfy today's data request, coherent transmission has to be used in such cables. The aim of this thesis is so to understand how to exploit these subsea DM links using coherent transmission technology, extending existing analytical results for UT to DM architectures using a simulative approach in order to extract meaningful informations and validate analytical models. The final scope is so to end up with a quick, handly QoT (Quality of Transmission) estimation that does not require time-consuming numerical simulations to be obtained.

Acknowledgements

First of all I would like to thank my supervisors Emanuele Virgillito and Vittorio Curri, with whom I had the pleasure to continue their outstanding past research work. Their guidance, expertise and holistic views on the field have been so fundamental and inspiring for me to grow technical competences as well as a general attitude to grasp the core of problems while abstracting the necessary tools to solve them.
I want also to thank Nokia team, collaborating with them has been a really enriching experience, allowing me to tackle practical challenges firsthand and gain a deeper understanding of real-world problems and their solutions.
Other thanks go to all my friends both from Licata and Torino, which made these university years further enjoyable.
Finally, I want to thank my family for their unwavering support throughout these years, making all the opportunities I have had possible.

Table of Contents

List of Tables

List of Figures

Acronyms

ASE
: Amplified Spontaneous Emission

B2B
: Back-To-Back

CuT
: Channel under Test

DCF
: Dispersion Compensating Fiber

DCU
: Dispersion Compensating Unit

DM
: Dispersion Managed

DP
: Double Polarization

DSP
: Digital Signal Processing

EDFA
: Erbium-Doped Fiber Amplifier

GN
: Gaussian-Noise

GSNR

Generalized Signal-to-Noise Ratio

IMDD

Intensity Modulation Direct Detection

LMF

Low Melting Fiber

NLI

Non-Linear Interference

NLSE

Non-Linear Schrodinger Equation

OLS

Optical Line System

OSNR

Optical Signal To Noise Ratio

PSD

Power Spectral Density

QoS

Quality-of-Service

QoT

Quality-of-Transmission

RP

Random Process

RV

Random Variable

SCI

Self-Channel Interference

SNR
: Signal-to-Noise Ratio

SPM
: Self-Phase Modulation

SSFM
: Split Step Fourier Method

XCI
: Cross-Channel Interference

XPM
: Cross-Phase Modulation

UT
: Uncompensated Transmission

WDM
: Wavelength Division Multiplexing

Chapter 1

Introduction and Fundamental Concepts

1.1 Introduction

This work is structured as follows: In Chapter 1 there are presented some of the most relevant optical fiber transmission physical concepts and impairments to comprehend the subsequent discussions. In Chapter 2 we will describe the fundamental ideas with proofs concerning the modeling used, extending the already existing mathematical tools for NLI evaluation in UT scenario to DM one. Chapter 3 will be dedicated to the explanation of simulative approach used: first we'll present simulator structure and features, and then the simulation strategies used to extract meaningful results to compare with out analytical modeling. Chapter 4 shows main results obtained comparing simulation data with analytical ones in order to validate the developed model and understand its accuracy and limits, and finally in Chapter 5 some conclusions and further ideas for future works and investigations are drew up.

1.2 Optical Fiber Trasmission Features

We will now review the main propagation impairments of the electromagnetic field in optical fibers that are relevant to the problems addressed in this thesis. Many of the reported topics are deeply described in [1].

1.2.1 Chromatic Dispersion

Chromatic dispersion is a phenomenon that makes different chromatic components propagate at different velocities. This can be mathematically seen writing the propagation expression in frequency domain:

$$E(z,\omega) = E(0,\omega)e^{-\alpha z}e^{-j\beta(\omega)z} \tag{1.1}$$

And observing that $\beta(\omega)$ is not a constant but a rather smooth function of ω. In order to understand how chromatic dispersion affects signal propagation, usually β is written in taylor series as:

$$\beta(\omega) = \beta_0 + \beta_1(\omega-\omega_0) + \frac{1}{2}\beta_2(\omega-\omega_0)^2 + \frac{1}{6}\beta_3(\omega-\omega_0)^3 + ... \tag{1.2}$$

To see the effect of main orders $\beta(\omega)$ components, is worth to write equation (1.1) as

$$E_R(\omega) = s_T(\omega-\omega_0)e^{-j\beta(\omega)z} \tag{1.3}$$

Here, we neglected $e^{-\alpha z}$ since does not depend on frequency and so does not introduce spectrum distortion, being just the same multiplicative constant for every ω. We consider just electric field at receiver $E_R(\omega)$, writing it depending on the transmitted field $E(0,\omega) = E_T(\omega) = s_T(\omega-\omega_0)$, where $s_T(\omega-\omega_0)$ is the modulated signal in frequency domain centered in ω_0.

If we truncate $\beta(\omega)$ at first order, so $\beta(\omega) \approx \beta_0 + \beta_1(\omega_0)\cdot(\omega-\omega_0)$, received field becomes:

$$E_R(\omega) = s_T(\omega-\omega_0)e^{-j[\beta_0+\beta_1\cdot(\omega-\omega_0)]z} \tag{1.4}$$

That in time domain corresponds to:

$$E_R(t) = s_T(t-\beta_1 z)e^{j\omega_0[t-\frac{\beta_0 z}{\omega_0}]} \tag{1.5}$$

So here we observe that, considering $\beta(\omega)$ as a linear function, resulting received field has its modulating envelope and carrier term "delayed" in time by two different factors based on β_1 and β_0 respectively. For that reason, $\frac{\beta_0 z}{\omega_0}$ is usually referred as phase delay τ_ϕ, while $\beta_1 z$ is referred as group delay τ_g. As it can be seen in equation (1.5), these parameters don't distort the spectrum.

Instead, considering $\beta(\omega)$ until its second order expansion, received field becomes:

$$E_R(\omega) = s_T(\omega-\omega_0)e^{-j\left[\beta_0+\beta_1\cdot(\omega-\omega_0)+\frac{\beta_2}{2}\cdot(\omega-\omega_0)^2\right]z} \tag{1.6}$$

For which, unfortunately, Inverse Fourier Transform cannot be computed analytically in general, but just for some particular cases. What is possible to do instead, is to divide spectrum in N sub-bands small enough to consider a linear $\beta(\omega)$, but different for each sub-band. So received field in that case is

$$E_R(\omega) = \sum_{i=-\frac{N}{2}}^{\frac{N}{2}} s_{T_i}(\omega - \omega_i) e^{j[\beta_0(\omega_i) + \beta_1(\omega_i)\cdot(\omega-\omega_i)]z} \tag{1.7}$$

Where β_0 and β_1 are in general different for each ω_i.
The field in time domain results to be:

$$E_R(t) = \sum_{i=-\frac{N}{2}}^{\frac{N}{2}} s_{T_i}(t - \tau_{g_i}) e^{j(t-\tau_{\phi_i})} \tag{1.8}$$

So each spectral component is delayed by a different group delay τ_{g_i}, that "spreads" signal pulse and a different phase delay τ_{ϕ_i}, which adds further distortion.

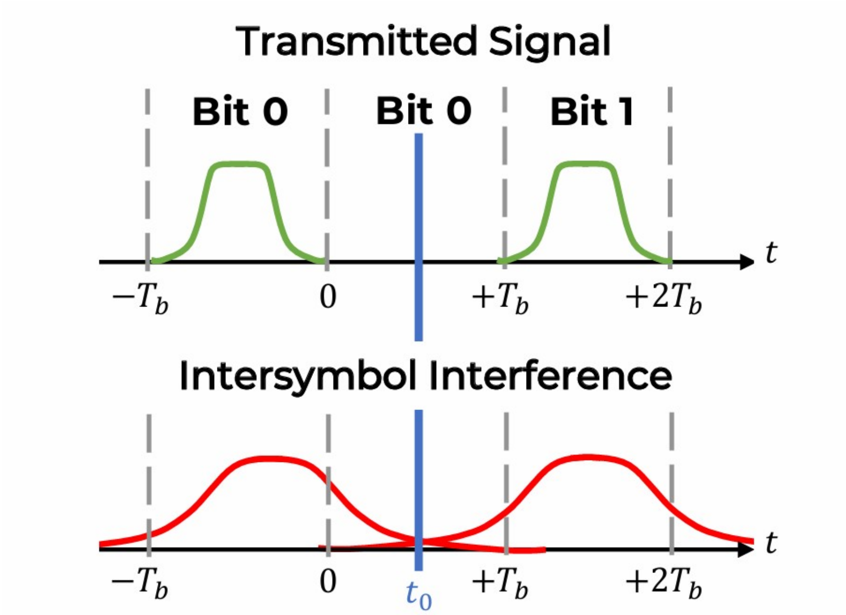

Figure 1.1: Effect of non-linear chromatic dispersion on TX signal in time domain

From a practical point of view, chromatic dispersion description based on (1.2) truncated to second order term is sufficient to provide a good approximation for propagation constant for WDM spectra occupying the roughly 5 THz of the C-Band. Taking into account further terms of Taylor expansion would be out of the scope for work presented. In particular, β_2 is the proper chromatic dispersion coefficient, expressed in ps/THz/km, which is commonly referred to in terms of the D parameter, which is basically the same thing except for being expressed in terms of wavelength rather than frequency, so it's measured as ps/nm/km.

1.2.2 Kerr Effect

Kerr effect is the main non-linear phenomenon to consider in field propagation in the fiber. It's physically observed that refractive index of the optical fiber core slightly changes proportionally to the injected field power instantaneously in time, following the law:

$$n(z,t) = n_L + n_2 \frac{P(z,t)}{A_{eff}} \tag{1.9}$$

where n_L is the conventional refractive index, n_2 is the "non-linear index coefficient" and A_{eff} is the optical mode "effective area", that corresponds roughly to the area where the mode is confined in the fiber (i.e. the area of the fiber core).

Usually, $\frac{\Delta n}{n_L}$ is very small (the order of magnitude is in the order of 10^{-11}), even at high power. So, the impact over propagation field, can be studied through a perturbative approach. Firstly, reminding that by definition

$$\beta = \frac{2\pi}{\lambda_{mode}} \approx \frac{2\pi}{\lambda} n \tag{1.10}$$

And then we observe that a Δn variation induces a $\Delta\beta$ variation as follows:

$$\Delta\beta = \frac{2\pi}{\lambda} \frac{n_2}{A_{eff}} P(z,t) = \gamma P(z,t) \tag{1.11}$$

Where

$$\gamma = \frac{2\pi}{\lambda} \frac{n_2}{A_{eff}} \tag{1.12}$$

is the Non-Linearity coefficient. Kerr effect consists so in power signal modulating the fiber β parameter. We remind that $P(z,t) = |E(z,t)|^2$, so from the optical field propagation, this is a Non-Linear relationship.

$\Delta\beta$ can be assumed as flat, broadband in frequency, according to the fact that refractive index changes instantaneously in time. So

$$\beta_{0,NL} = \beta_0 + \Delta\beta. \tag{1.13}$$

1.2.3 Non-linear Schrodinger Equation

Optical field propagation equation can be derived from Maxwell equations with proper boundary conditions. The equation in its general form (in frequency domain) is:

$$\frac{\partial E(z,\omega)}{\partial z} = \left[-\alpha - j\beta(\omega)\right] E(z,\omega) \tag{1.14}$$

In previous sections, we have seen that $\beta(\omega)$ actually includes dispersion and Kerr Effect contributions, so we have to insert explicitely them in the propagation equation. In order to do that, we recall the Taylor series expansion of $\beta(\omega)$ as in (1.2), centering it around the carrier frequency (in the following we consider the complex envelope of $E(z,t)$, so carrier frequency coincides with the origin of frequency axis, $\omega_0 = 0$). What we obtain is:

$$\frac{\partial E(z,\omega)}{\partial z} = \left[-\alpha - j\left((\beta_0 + \Delta\beta) + \beta_1\omega + \frac{1}{2}\beta_2\omega^2\right)\right] E(z,\omega) \tag{1.15}$$

By taking the Inverse Fourier Transform and recalling that

$$\mathcal{F}^{-1}[(j\omega)^n] = \frac{\partial^n}{\partial t^n}, \tag{1.16}$$

The equation become, in the time domain:

$$\frac{\partial E(z,t)}{\partial z} = -\alpha E(z,t) - j\frac{\beta_2}{2}\frac{\partial^2 E(z,t)}{\partial t^2} - j\gamma|E(z,t)|^2 E(z,t) \tag{1.17}$$

where we neglected β_0 and β_1 terms, deleting respectively a phase shift and a group delay since none of them distort the signal. Here $-\alpha E(z,t)$ is simply a loss term, $-j\frac{\beta_2}{2}\frac{\partial^2 E(z,t)}{\partial t^2}$ accounts for dispersion and $-j\gamma|E(z,t)|^2 E(z,t)$ represents Kerr effect term, which is clearly non-linear. This term is so the cause of non-linearity noise which affects the system, that is the estimation target of the presented work. A solution for (1.17) is carried out by GN Model in UT for a gaussian-distributed WDM spectrum, and it's presented in the next section.

1.2.4 GN model

GN model is the model on which we'll rely on for estimation of pure Non-Linear Interference power introduced by each span. It relies on the following hypotheses on propagating signal:

- It is a zero-mean complex Gaussian RP with uncorrelated phase and quadrature components

- It is periodic of period T_0, where T_0 is an integer multiple of the symbol duration T_s
- Its average PSD is shaped according to that of an actual WDM signal $\sqrt{G_{TX}(f)}$

In order to satisfy these conditions, signal model $E(t)$ is based on a filtered complex periodic white Gaussian noise (PWGN) process, as follows:

$$PWGN(f) = \sqrt{f_0} \sum_{n=-\infty}^{\infty} \xi_n \delta(f - nf_0) \tag{1.18}$$

where where the ξ_n's are complex Gaussian RVs of unit variance, independent of one another. Given the transfer function

$$H(f) = \sqrt{G_{TX}(f)} \tag{1.19}$$

propagating field considered will be

$$E(f) = PWGN(f) \cdot H(f) = \sqrt{f_0 \cdot G_{TX}(f)} \sum_{n=-\infty}^{\infty} \xi_n \delta(f - nf_0) \tag{1.20}$$

We can observe that with this signal model we have a gaussian distributed WDM spectrum, this is called gaussianization hypothesis. Actually, real world signals usually don't present such distribution but tend to it as they accumulate chromatic dispersion along the optical link. This is the reason why GN model provides a conservative, worst case estimation of Non-Linear interference. That final estimation is obtained inputting (1.20) in NLSE and carrying out the mathematical computation, that is done in [2]. This computation leads to spectrally disaggregated result: final NLI estimation is obtained as sum of SCI (Self-Channel Interference) and all XCI (Cross-Channel Interference) components where:

- SCI represents the CuT interfering on itself
- XCI_k represents the $k-th$ channel interfering with CuT

Since we'll largerly deal with systems in which SCI and XCI will be analyzed, it is convenient to name properly the considered channels: we will refer to the CuT as *probe* and to the $k-th$ channel interfering with it as *pump*. So, the equations that come out from GN model for SCI and XCI power are:

$$P_{SCI} = \eta_{SCI} P_{probe}^3 \tag{1.21}$$

in the case of Self-Channel-Interference and

$$P_{XCI,k} = \eta_{XCI,k} P_{probe} P^2_{pump_k} \tag{1.22}$$

in the case of Cross-Channel-Interference for the pump number k. We point out that the case $k = 0$ corresponds to SCI. Each η_{SCI} and $\eta_{XCI,k}$ is usually referred as Normalized NLI.

Here, the pure NLI power efficiencies η_{SCI} and $\eta_{XCI,k}$ result in

$$\eta_{SCI} = \frac{16}{27}\gamma^2 L^2_{eff} N_s \frac{\operatorname{asinh}\left(\frac{\pi}{2}|\beta_2|(2\alpha)^{-1} B^2_{ch,i}\right)}{2\pi|\beta_2|(2\alpha)^{-1}}$$

$$\begin{aligned}\eta_{XCI,i,n} = 2 \cdot \frac{16}{27}\frac{\gamma^2 L^2_{eff} N_s}{4\pi|\beta_2|(2\alpha)^{-1}} \Bigg[& \operatorname{asinh}\left(\pi^2|\beta_2|(2\alpha)^{-1}\left[f_{ch,n} - f_{ch,i} + \frac{B_{ch,n}}{2}\right] B_{ch,i}\right) \\ & - \operatorname{asinh}\left(\pi^2|\beta_2|(2\alpha)^{-1}\left[f_{ch,n} - f_{ch,i} - \frac{B_{ch,n}}{2}\right] B_{ch,i}\right)\Bigg]\end{aligned} \tag{1.23}$$

Where:

- i and n are channel indexes
- N_s is the number of spans
- $f_{ch,i}$ is the central frequency of channel i
- $B_{ch,i}$ is the bandwidth of channel i
- $\gamma \left[\frac{1}{W \cdot km}\right]$ is the non-linearity coefficient
- $\beta_2 \left[\frac{ps}{nm \cdot km}\right]$ is the second order group velocity dispersion
- $\alpha \left[\frac{1}{km}\right]$ is the fiber attenuation coefficient
- L_{eff} $[km]$ is the fiber effective length, defined as $\left(\frac{1-e^{\alpha L}}{\alpha}\right)$

The full NLI evaluation is obtained summing together equations (1.21) and (1.22) as:

$$P_{NLI} = P_{SCI} + 2 \cdot \sum_{k=1}^{\frac{N_{ch}}{2}} P_{XCI,k} \tag{1.24}$$

considering a symmetric spetrum with respect y-axis composed by an odd number of channels N_{ch} (which is a configuration largely used, even in this work).

1.2.5 SNR as QoT metric

In general, in optical communication systems, Bit Error Rate before application of Forward Error Correction algorithm (pre-FEC BER) is the main quality metric for performances evaluation. BER is a known function of SNR, which different curves are generated based only on the modulation format used (we can see example of BER vs SNR curves in Figure 1.2).

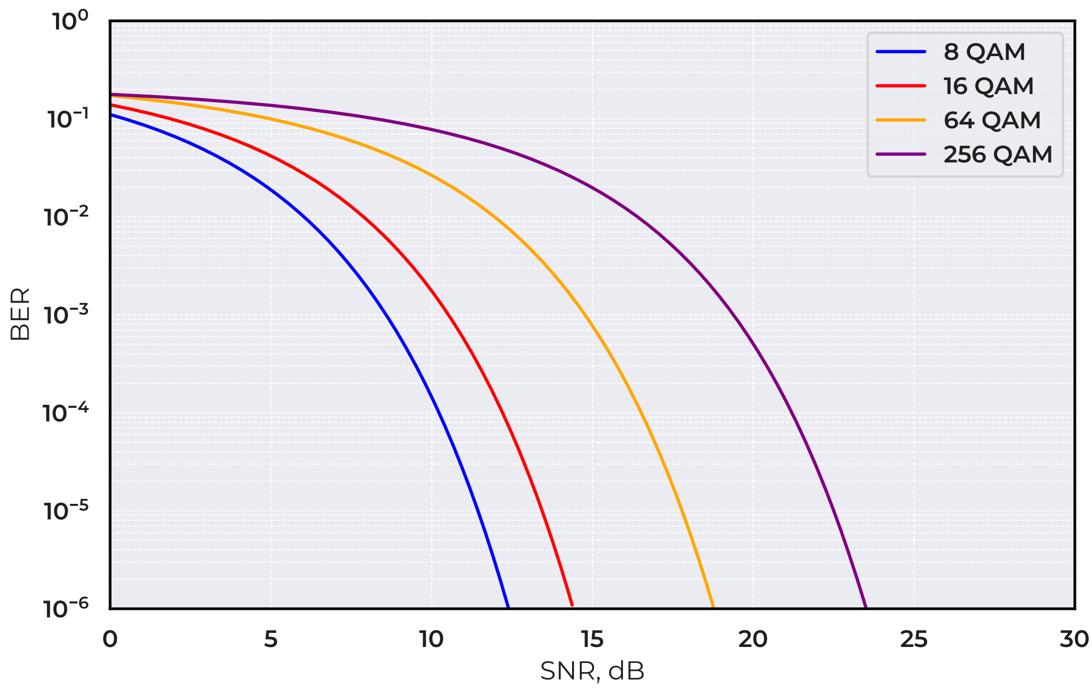

Figure 1.2: BER vs SNR curves example

So our final quality metric is SNR. Actually, in optical systems SNR takes into account different noise contributions and it's referred as GSNR (Generalized Signal-to-Noise Ratio):

$$GSNR = \frac{P_{sig}}{P_{NLI} + P_{ASE}} \tag{1.25}$$

Where P_{NLI} is the power of Non-Linear interference noise introduced by Kerr-Effect and P_{ASE} is the power of Amplified Spontaneous Emission noise, that is intrinsic in any EDFA device, for which evaluation, we recall the known formula

$$P_{ASE} = h\nu(G - 1)BF \tag{1.26}$$

Where h is the Planck constant, ν is the photons frequency, B is the bandwidth of the CuT and G and F are respectively the Gain and Noise Figure of EDFA amplifiers used. Formula (1.26) is valid in any context and it's related only to noise introduced by optical amplifiers, while P_{NLI} depends on Non-Linear disturbance introduced by Kerr effect. So they're two completely separated problem and our investigation will be focused just on P_{NLI} evaluation in Dispersion-Managed scenario.

So, at this point, we can decompose GSNR in the two SNRs contributions:

$$OSNR = \frac{P_{sig}}{P_{ASE}}, \qquad SNR_{NLI} = \frac{P_{sig}}{P_{NLI}} \tag{1.27}$$

That results in:

$$\frac{1}{GSNR} = \frac{1}{SNR_{NLI}} + \frac{1}{OSNR} \tag{1.28}$$

For what concerns SNR_{NLI} evaluation in spectral disaggregated approach, recalling equations (1.21) and (1.22), we can write:

$$SNR_{SCI} = \frac{P_{probe}}{\eta_{SCI} P_{probe}^3} = \frac{1}{\eta_{SCI} P_{probe}^2} \tag{1.29}$$

$$SNR_{XCI,k} = \frac{P_{probe}}{\eta_{XCI,k} P_{probe} P_{pump,k}^2} = \frac{1}{\eta_{XCI,k} P_{pump,k}^2} \tag{1.30}$$

Actually, we will consider WDM spectra with N_{ch} channels at the same power P_{ch} (which is a widely common configuration), in that case, overall SNR_{NLI} consists in:

$$\frac{1}{SNR_{NLI}} = \frac{1}{SNR_{SCI}} + \sum_{k=1}^{N_{pumps}} \frac{1}{SNR_{XCI,k}} = P_{ch}^2 \left(\eta_{SCI} + \sum_{k=1}^{N_{pumps}} \eta_{XCI,k} \right) \tag{1.31}$$

So, calling sum of normalized SCI and XCIs as η, we obtain:

$$SNR_{NLI} = \frac{1}{\eta P_{ch}^2} \tag{1.32}$$

Chapter 2

Analytical Modeling in Dispersion-Managed Scenario

2.1 Overview: Spectral and Spatial Disaggregation

Optical field, as seen, propagates itself along the fiber following NLSE. Although we have seen GN model solution, which holds for a gaussian-distributed WDM spectrum, a general solution for any $E(z,t)$ obtained solving NLSE (aggregated approach) does not exist, but in general ground truth results can be obtained through numerical simulations (as we will see in the next chapter). Even if optical field propagation is an intrinsically aggregated phenomenon, our model will rely instead on the concepts of spectral and spatial disaggregation, getting a quantitative idea of how much the disaggregation paradigm can well-approximate aggregated results.

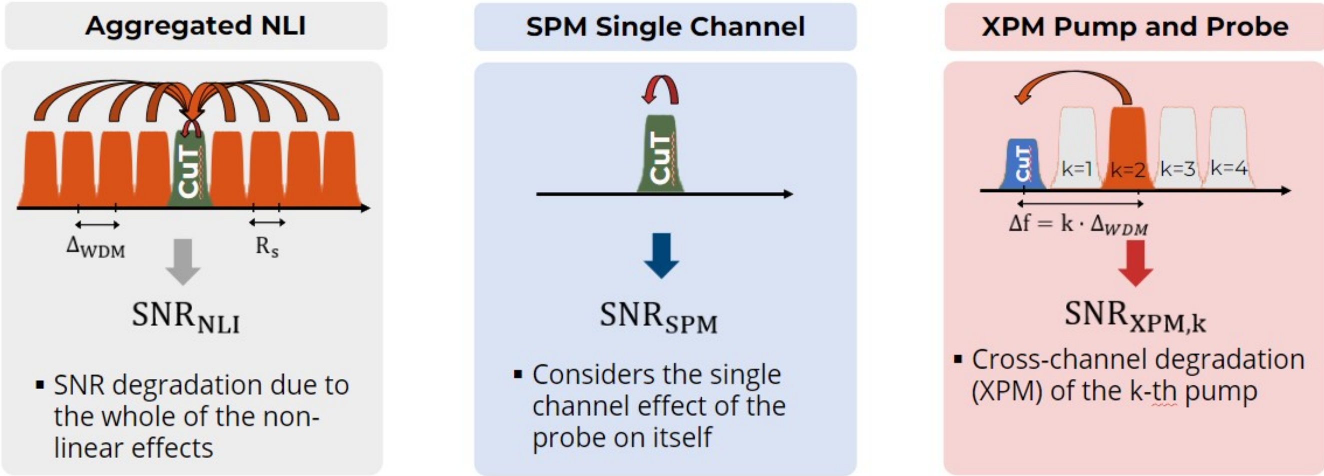

Figure 2.1

- Spectral Disaggregation is well expressed by the formula:

$$\frac{1}{SNR_{NLI}} = \frac{1}{SNR_{SPM}} + \sum_{k=1}^{N_p} \frac{1}{SNR_{XPM,k}} \tag{2.1}$$

  Where k is the index of $k-th$ pump. So Spectral Disaggregation is verified if full spectral load NLI obtained by aggregated solution can be obtained by summing up SCI and XCI_k contributions.

- Spatial Disaggregation, instead, is defined as:

$$\Delta SNR_{SCI,i} = \frac{P_{ch}}{\Delta P_{SCI,i}}$$

$$\Delta SNR_{XCI,k,i} = \frac{P_{ch}}{\Delta P_{XCI,k,i}} \tag{2.2}$$

  Where

$$\Delta P_{SCI,i} = \sigma^2_{SCI,i} + 2\sum_{j=1}^{i-1} C_{ij}\sigma_{SCI,i}\sigma_{SCI,j}$$

$$\Delta P_{XCI,i} = \sigma^2_{XCI,i} + 2\sum_{j=1}^{i-1} C_{ij}\sigma_{XCI,i}\sigma_{XCI,j} \tag{2.3}$$

  Where $\sigma^2_{SCI,i}$ and $\sigma^2_{XCI,i}$ are respectively SCI and XCI powers contributions introduced by $i-th$ span, C_{ij} is the Correlation Coefficient that accounts for the accumulated dispersion between span i and span j, and so $\Delta P_{SCI,i}$ and $\Delta P_{XCI,i}$ are respectively total SCI/XCI power increments introduced by span i. Formulas (2.3) represent the innovation with respect the already existing approaches and will be mathematically proved in the next section.

In general, it's important to have a spectrally disaggregated model since we can split each Non-Linear Interference spectral contribution getting the amount of NLI that belongs to each portion of occupied bandwidth in a multiple channel propagation scenario. On the other hand, it's important to have a spatially disaggregated model in order to separate coherency contributions span by span getting a quantitative idea about spatial memory of the system.

The non-linear noise generation is spatially disaggregated when the amount of noise introduced by each fiber span does not depend on the previous propagation history. This has been demonstrated to be substantially true in UT systems. In dispersion managed systems instead, the small amount of chromatic dispersion left after inline compensation units introduced a certain amount of coherency between the noise contributions introduced by different spans which breaks in general the strict spatial disaggregation. However, the coherency contributions between different spans can be disaggregated in a wider sense in order to estimate the spatial memory of the coherent accumulaton phenomenon.

2.2 Model Derivation

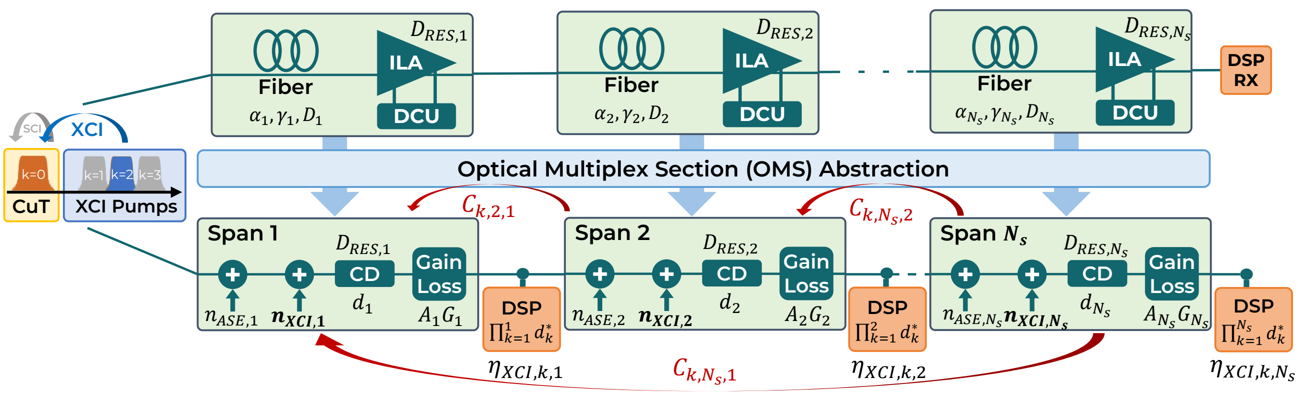

Figure 2.2: General system topology abstraction

In order to properly develop an analytical model for DM scenario, we consider a general system composed by N_s equal spans, each composed by:

- ASE noise source
- NLI source $n_i(t)$ modeled as Additive RP
- A piece of fiber with loss A_i and dispersion d_i
- EDFA amplifier with gain G_i

The traditional NLI modelling based on the GN model considers the system aggregated in space and frequency. Here instead, we treat the NLI as a random noise process introduced equivalently at each span input, as long as the fiber length exceeds the effective length. The coherency phenomenon then arises at the receiver by the cross-correlation terms of different span noise fields.

At the end of each span, chromatic dispersion compensation is performed by DSP, which acts multiplying the span output signal by $\prod_{k=1}^{i} d_k^*$, holding the property $d_k^* d_k = 1$.

Calling the XCI/SCI noise at the end of $i-th$ span as $\overline{n}_i(t)$, we can write, by induction

$$\overline{n}_1 = \sqrt{A_1 G_1} n_1$$

$$\overline{n}_2 = \sqrt{A_2 G_2}\left(\sqrt{A_1 G_1} n_1 + d_1^* n_2\right)$$

$$\overline{n}_3 = \sqrt{A_3 G_3}\left(\sqrt{A_2 G_2 A_1 G_1} n_1 + \sqrt{A_2 G_2} d_1^* n_2 + d_1^* d_2^* n_3\right) \tag{2.4}$$

So the general expression for $\overline{n}_i$ is:

$$\overline{n}_i(t) = \sum_{k=1}^{i}\left(n_k(t) \cdot \prod_{j=k}^{i} \sqrt{A_j G_j} \cdot \prod_{n=1}^{k-1} d_n^*\right) \tag{2.5}$$

That can also be written as:

$$\overline{n}_i(t) = \sqrt{A_i G_i}\left(\overline{n}_{i-1}(t) + n_i(t) \cdot \prod_{j=1}^{i-1} d_j^*\right) \tag{2.6}$$

The power of XCI/SCI noise at the end of $i-th$ span is, by definition:

$$P_{\overline{n}_i}(t) = \mathbb{E}\left[|\overline{n}_i(t)|^2\right] \tag{2.7}$$

So we develop the computation putting (2.6) into (2.7), leaving implicit dependency from time t in order to have a more compact notation::

$$P_{\overline{n}_i} = \mathbb{E}\left[\left|\sqrt{A_i G_i}\left(\overline{n}_{i-1} + n_i \cdot \prod_{j=1}^{i-1} d_j^*\right)\right|^2\right]$$

$$P_{\overline{n}_i} = A_i G_i \cdot \mathbb{E}\left[\left(\overline{n}_{i-1} + n_i \cdot \prod_{j=1}^{i-1} d_j^*\right) \cdot \left(\overline{n}_{i-1} + n_i \cdot \prod_{l=1}^{i-1} d_l^*\right)^*\right]$$

$$P_{\overline{n}_i} = A_i G_i \cdot \mathbb{E}\left[|\overline{n}_{i-1}|^2 + \overline{n}_{i-1} n_i^* \prod_{j=1}^{i-1} d_j + \overline{n}_{i-1}^* n_i \prod_{l=1}^{i-1} d_l^* + |n_i|^2\right] \tag{2.8}$$

Since $\mathbb{E}$ is a linear operator, we can separately compute it on each single term of the sum, and given the definition (2.7), we can immediately determine:

$$\mathbb{E}\left[|\overline{n}_{i-1}|^2\right] = P_{\overline{n}_{i-1}}$$

$$\mathbb{E}\left[|n_i|^2\right] = \sigma_i^2 \tag{2.9}$$

Where $P_{\overline{n}_{i-1}}$ is the total accumulated power until the span $i-1$ and σ_i^2 is the pure NLI contribution introduced by span i alone, without other spans contribution.

Now we better investigate the remaining terms:

$$\mathbb{E}\left[\overline{n}_{i-1} n_i^* \prod_{j=1}^{i-1} d_j + \overline{n}_{i-1}^* n_i \prod_{l=1}^{i-1} d_l^*\right] \tag{2.10}$$

Substituting (2.5) in (2.10), we obtain

$$\mathbb{E}\left[\sum_{k=1}^{i-1}\left(n_k \cdot \prod_{j=k}^{i-1}\sqrt{A_i G_i} \cdot \prod_{n=1}^{k-1} d_n^*\right) n_i^* \prod_{j=1}^{i-1} d_j + \sum_{k=1}^{i-1}\left(n_k \cdot \prod_{j=k}^{i-1}\sqrt{A_j G_j} \cdot \prod_{n=1}^{k-1} d_n^*\right)^* n_i \prod_{l=1}^{i-1} d_l^*\right] \tag{2.11}$$

We can compact the dispersion terms as

$$\prod_{n=1}^{k-1} d_n^* \cdot \prod_{j=1}^{i-1} d_j = d_1^* d_2^* \ldots d_{k-1}^* \cdot d_1 d_2 \ldots d_{k-1} d_k \ldots d_{i-1} = d_k \ldots d_{i-1} = \prod_{j=k}^{i-1} d_j$$

$$\prod_{n=1}^{k-1} d_n \cdot \prod_{l=1}^{i-1} d_l^* = d_1 d_2 ... d_{k-1} \cdot d_1^* d_2^* ... d_{k-1}^* d_k^* ... d_{i-1}^* = d_k^* ... d_{i-1}^* = \prod_{j=k}^{i-1} d_l^* \tag{2.12}$$

So, putting (2.12) in (2.11) we have:

$$\prod_{j=k}^{i-1} \sqrt{A_j G_j} \cdot \sum_{k=1}^{i-1} \mathbb{E}\left[n_k n_i^* \prod_{j=k}^{i-1} d_j + n_k^* n_i \prod_{j=k}^{i-1} d_j^* \right] \tag{2.13}$$

The term $\mathbb{E}\left[n_k n_i^* \prod_{j=k}^{i-1} d_j + n_k^* n_i \prod_{j=k}^{i-1} d_j^*\right]$ can be proved to be equal to (Appendix A):

$$2\mathbb{E}\left[\Re\left(n_i n_k^* \prod_{j=k}^{i-1} d_j^*\right)\right] \tag{2.14}$$

which represents the additional coherency power introduced by span couple i and j. We will refer to it as $2\sigma_{ij}$.

So now we can write the entire NLI Power accumulated at the end of span i:

$$P_{\overline{n}_i} = A_i G_i \left(P_{\overline{n}_{i-1}} + \sigma_i^2 + 2\sum_{j=1}^{i-1} \sigma_{ij} \cdot \prod_{k=j}^{i-1} \sqrt{A_j G_j} \right)$$

$$P_{\overline{n}_i} = A_i G_i \left(P_{\overline{n}_{i-1}} + \Delta P_{\overline{n}_i} \right) \tag{2.15}$$

Where $\Delta P_{\overline{n}_i}$ is the NLI Power increment between span i and span $i-1$. It's composed by two terms: σ_i^2, that is the pure noise power introduced by $i-th$ span alone and $2\sum_{j=1}^{i-1} \sigma_{ij} \cdot \prod_{k=j}^{i-1} \sqrt{A_j G_j}$, that expresses coherency power of span i with all the previous spans.

Coherency power, as it can be seen in (2.14), is just a function of random noise and accumulated dispersion. It can be approximated as $\sigma_{ij} \approx C_{i,j}\sigma_i\sigma_j$, that is a convenient form since we separate the contribution of pure noise power terms (under square root) and a correlation coefficient $C_{i,j}$ that takes into account the coherency between span i and span j, for which $|C_{i,j}| < 1$ holds. We now focus on transparent case $\left(G_i = \frac{1}{A_i}\right)$, so NLI power noise increment per span become: $\Delta P_{\overline{n}_i}$:

$$\Delta P_{\overline{n}_i} = \sigma_i^2 + 2\sum_{j=1}^{i-1} C_{ij}\sigma_i\sigma_j \tag{2.16}$$

which corresponds to equations 2.3. For what concerns evaluation of each σ_i^2, we rely on SCI and XCI power formulas (1.21) and (1.22).

2.3 Correlation Coefficients Estimation: Machine Learning Approach

Looking at formula (2.16), the only variable for which we lack an analytical closed-form estimation is C_{ij}. Of course we can estimate it running a bunch of spatially disaggregated simulations, but as it will be explained in detail in section 3.2.2, this is in general a non feasible procedure.

What we consider instead as a quick method is a Machine Learning approach: the estimation translates basically in a regression problem on C_{ij}, that is modeled as a function of various parameters:

$$C_{ij} = f(\beta_{2,i}, \beta_{2,j}, \beta_{2,acc,i}, \beta_{2,acc,j,}, \beta_{2,acc,(i,j)}, \alpha_i, \alpha_j, \gamma_i, \gamma_j, Rs, \Delta f) \tag{2.17}$$

Here:

- $\beta_{2,acc,i} = \sum_{k=1}^{i} \beta_{2,k} L_{s,k}$ is dispersion accumulated from the beginning of the link to span i
- $\beta_{2,acc,(i,j)} = \sum_{k=j}^{i} \beta_{2,k} L_{s,k}$ is dispersion accumulated from span j to span i
- Δf is the frequency spacing between pump and probe (we remark that correlation coefficients, as they are defined, makes sense only in a pump and probe context, so they'll be calculated just in such simulations. Hence Δf definition is not ambiguous).

In [3] has been shown that C_{ij} is mainly a function of $\beta_{2,acc,(i,j)}$ in an uniform context where chromatic dispersion compensation is applied periodically in each span with the same value via DCUs. However, even if the accumulated dispersion between the two SuT is fundamental to address the phenomenon, C_{ij} is generally a function of many parameters, especially due to the fact that dispersion compensation may not necessarily be performed by DCUs but also by DCFs (in chapter 4 about validation, we will test the model on a system that relies on such elements), that are physical fiber with dispersion coefficient usually with opposite sign with respect the total dispersion accumulated in previous spans. As fibers, DCFs intrinsecally introduce also non linearity, so Machine Learning model has to take into account more parameters to address correctly the phenomenon in general. Chosen model for this problem is Random Forest with $N_{estimators} = 100$, which has been trained on a dataset consisting in a bunch of simulation data containing various scenarios with both DCFs and DCUs, mixed physical fiber parameters (even dispersion, resulting in different dispersion maps) and also different spectrum parameters, in order to generalize as much as possible the model predictions. Final performances of Random Forest are observable in Figure 2.3, with R^2 Score of 0.9962 and 0.0004 MSE.

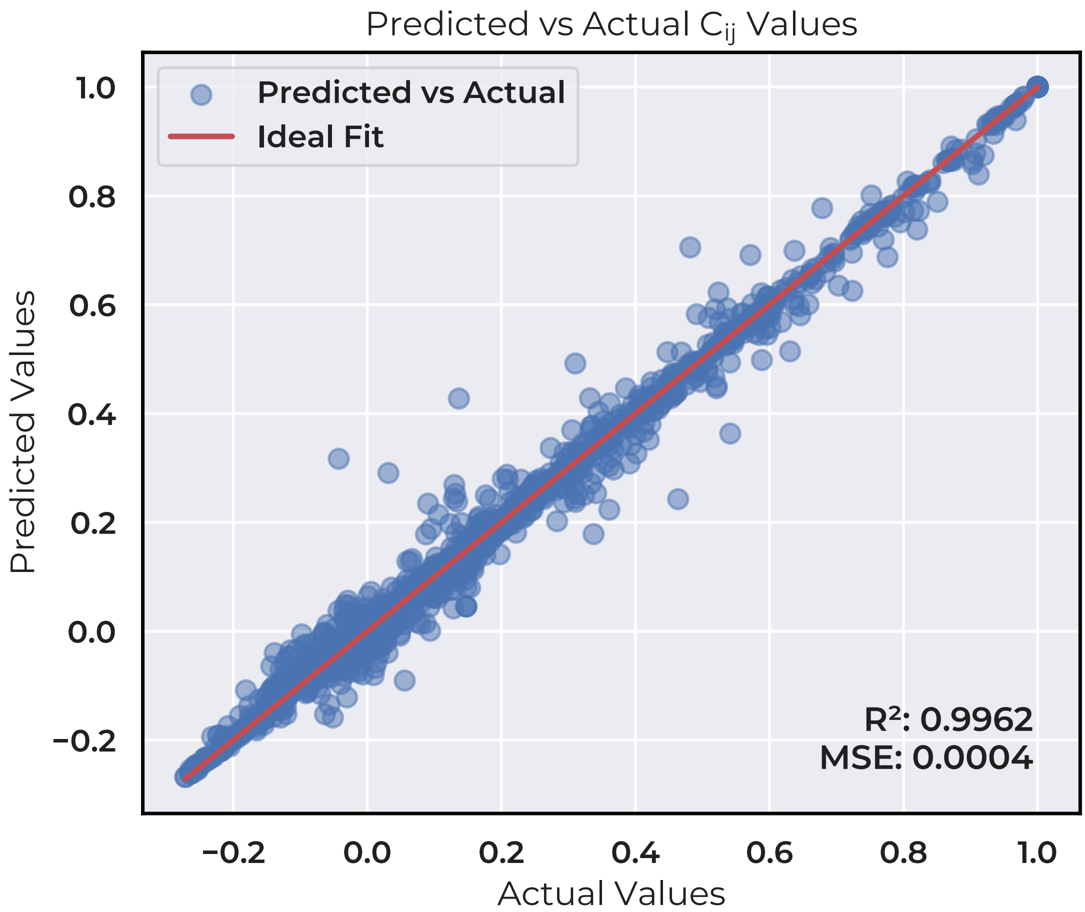

Figure 2.3: Random Forest fitting for correlation coefficients

Chapter 3

Split Step Fourier Method-Based Simulator

3.1 General Simulator Description

In order to generate numerical results to compare with our modeling, a powerful MATLAB-based simulator is used. That simulator is able to emulate signal propagation in a customized optical line system and outputting metrics of interest, that will be used for data post processing. In order to describe the system to be simulated, the simulator takes in input 4 json files:

- spectral_information: definition and settings for signal used through its spectral parameters.
- line: describes the topology of network element-by-element (SMFs, DCFs, DCUs, EDFAs, ...) with all their internal parameters. A remarkable point that will be useful in the following, consists in the possibility to specify specify in which spans Kerr effect is on.
- receiver: contains the chain of stages composing the receiver for a given CuT, similarly to the line json.
- ssfm_parameters: sets simulation parameters and polynomial degree of randomizer used.

Listing 3.1: Sample JSON code for spectral information description

```
{
    "spectral_info": {
        "frequency": [194.00e12, 194.150e12],
        "baud_rate": 65e9,
        "slot_width": 75e9,
        "channel_powers_dBm": [-18.0, 0.0],
        "modulation_format": 2,
        "psnm_predistortion": 0,
        "predistortion_ref_wavelength": 1.55e-06,
        "predistortion_b2_ref_frequency": "channel_center",
        "shaping_filter": [
            "rrc",
            0.0625,
            64
        ]
    }
}
```

We can see in Listing 3.1 an example of JSON file configuration for a spectrum composed by 2 channels root raised cosine-shaped, where the CuT is kept lower in power with respect the other one. This kind of configuration will be addressed as "pump and probe" one.

Listing 3.2: Sample JSON code for line description

```
{
    "type_variety": "ols",
    "repetitions": 20,
    "kerr_on": [
        2,
        19
    ],
    "elements": [
        {
            "uid": "NZDSF",
            "type": "Fiber",
            "type_variety": "NZDSF",
            "span_id": 1,
            "params": {
                "length": 80,
                "loss_coef": 0.2,
                "length_units": "km",
                "con_in": 0,
                "con_out": 0,
                "dispersion": 4e-06,
                "gamma": 0.00127,
                "pmd_coef": 0.1,
                "dispersion_ref_wavelength": 1.55e-06
            },
            "save": false,
            "dispersion_compensation": true
        },
        {
            "uid": "DCU",
            "type": "Fiber",
            "type_variety": "dispersive_element",
            "span_id": 1,
            "params": {
                "dispersion_accumulated": -0.28,
                "dispersion_ref_wavelength": 1.55e-06
            },
            "save": false,
            "dispersion_compensation": true
        },
        {
            "uid": "EDFA",
            "type": "Edfa",
            "type_variety": "EDFA17",
            "span_id": 1,
            "operational": {
                "gain_target": 16.0,
                "delta_p": null,
                "tilt_target": 0,
```

```
                    "out_voa": 0,
                    "nf_db": 5
                },
                "save": true,
                "dispersion_compensation": true
            }
        ]
}
```

In Listing 3.2 there is reported an example json configuration for a link composed by a fiber, DCU and EDFA, repeated 20 times. Here Kerr effect is active only in spans 2 and 19. This will be a very important configuration that will be used in the following to analyze the coherency correlation between two spans.

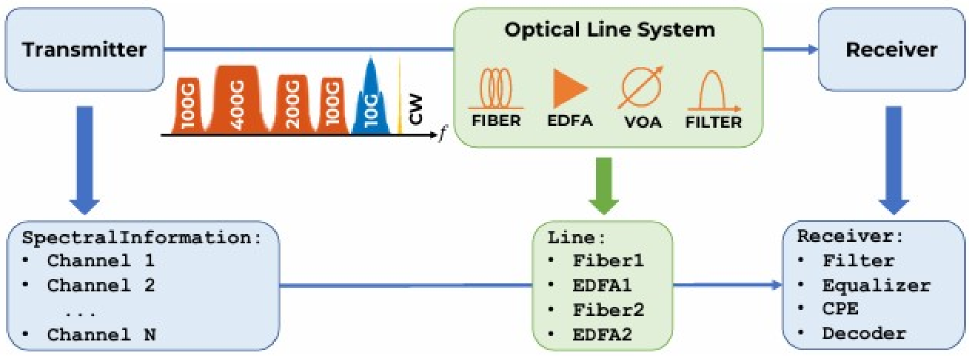

Figure 3.1: Simulator Structure

The simulator relies on Split-Step-Fourier-Method. It consists basically in a particular way to solve numerically NLSE, which cannot be solved analytically for every $E(z, t)$, except for particular and non-realistic cases like non-dispersive fibers or with absence of non-linearities. Here we can write in a more convenient way the right part of the equality: a linear operator $\mathcal{L}$ that accounts for fiber loss and dispersion in the frequency domain and a non-linear operator $\mathcal{N}$ applying Kerr effect in the time domain (since Fourier transform of Kerr effect does not have a closed form solution in general), resulting in

$$\frac{\partial E(z, \omega)}{\partial z} = \mathcal{L}[E(z, \omega)] + \mathcal{F}\{\mathcal{N}[E(z, t)]\} \tag{3.1}$$

The idea behind SSFM is that, despite $\mathcal{L}$ and $\mathcal{N}$ act simultaneously in the actual physical process, they can be treated as independent by applying them separately (as shown in Figure 3.2). This assumption becomes increasingly accurate as the fiber segment dz approaches zero.

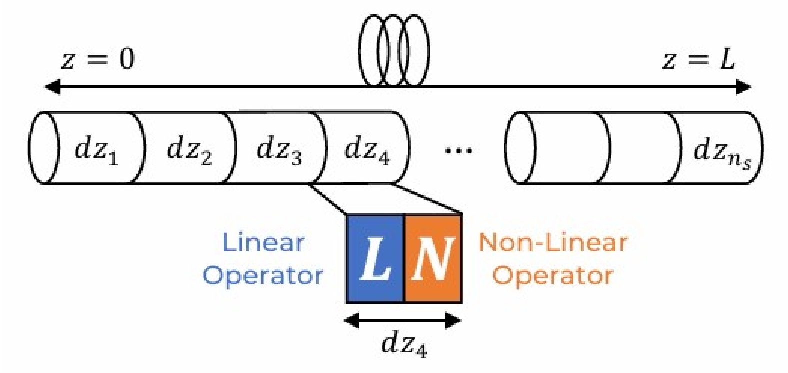

Figure 3.2: Scheme of the Split-Step Fourier Method. The linear L and non-linear N operators are applied separately in each dz step.

Despite such SSFM-based simulator produces totally reliable results, the main problem in using it in real time scenarios is that of intense computational requirements, since it requires Graphical Processing Unit (GPU) and even with it, simulation time is totally non negligible: for a WDM signal composed by few channels (9 to 15) occupying barely half THz bandwidth in a link around 1000 km long (similar to scenario that we will analyze in validation section in chapter 4), simulation time required is in the order of days. This obviously gets worse with increasing number of channels (due to simulation bandwidth growth) and/or link length (due to number of computations required) making the process unfeasible sometimes, so such a simulator cannot be used for real time deployment, but is extremely useful as a support to develop a closed form model to work in such conditions.

3.2 Simulation Strategies

Now we will present simulation techniques used in order to obtain ground truth results about spectral and spatial disaggregation to compare with outcomes of our modeling. All the simulations presented are loaded in a Python-based post processing software, which extract metrics of interest giving the possibility to execute further computations on them. For what concerns SCI, simulations are loaded as they are without modifications, differently from XCI ones: in that case, pump and probe simulations are run, where the pump is launched at its nominal power and probe/CuT is set to a way lower power to keep low residual SCI effect. Anyway, in order to be sure to see only XCI without any covering from SCI in such simulations, we perform the operation:

$$\frac{1}{SNR_{XCI,k}} = \frac{1}{SNR_{SXCI,k}} - \frac{1}{SNR_{SCI}} \tag{3.2}$$

Where

$$\frac{1}{SNR_{SXCI,k}} = \eta_{SCI} P_{probe}^2 + \eta_{XCI,k} P_{pump}^2, \tag{3.3}$$

corresponds to output raw SNR value from pump and probe simulation for k-th pump. We recall SNR_{SCI} and $SNR_{XCI,k}$ expressions in equations (1.29) and (1.30).

3.2.1 Spectral Disaggregation

To test that spectral disaggregation is working, we have to verify equation (2.1), so we take:

- A simulation in which we propagate N_{ch} aggregated channels with the same power, that corresponds to ourput propagation ground truth. We will refer to this simulation as the *multichannel* one.

- A set of simulations in which we take separately each SCI/XCI $k-th$ component out of N_{pumps}. As mentioned before, in SCI case, we propagate just the CuT, while in XCI case we propagate the interested $k-th$ pump together with CuT, which is kept low in power. These will be referred as *pump and probe* simulations.

3.2.2 Spatial Disaggregation

In order to test spatial disaggregation, we have to verify equations (2.3), so we have to check consistency between actual pump and probe SCI/XCIs results and its reconstruction done using such formulas. Therefore, we have to take two simulations set:

- The actual pump and probe SCI/XCI, with Kerr-Effect turned on on all the spans. These simulations are equivalent to the set presented in second point of section 3.2.1.

- A bunch of simulations where:

  - Kerr-Effect is turned ON on one span per simulation, in order to estimate "pure" non-linear contribution σ_i^2 introduced by span i alone.

– Kerr-Effect is turned ON on two spans per simulation, consisting in the i-th Span under Test and all the previous j-th spans, one per time. So in order to estimate coherent NLI at span i (with all the correlation coefficients needed), we need all the simulations in which we turn on Kerr-Effect in Spans (i, 1), (i, 2), ..., (i, j), ..., (i, i-1) (Figure 3.3).

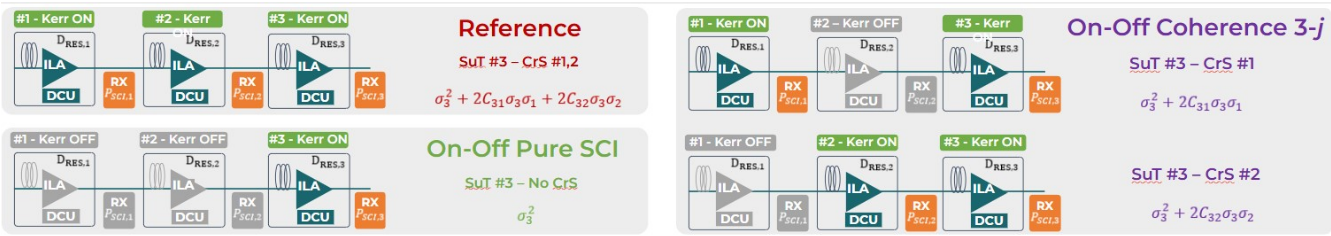

Figure 3.3: Spatial Disaggregation simulation method

Following this procedure we observe that, just for spatial disaggregation simulations, we have to run $N_{pumps} \cdot \sum_{n=1}^{N_{spans}} n$ simulations, which simulation time increases furtherly with pump and probe spectral distance due to larger simulation bandwidth deployed. So this procedure is useful at a validation and modeling stage, but is totally unfeasible as the numbers of spans and optical channels increase: hence it remarks the need to have a closed-form model that does not rely on SSFM simulations.

Chapter 4

Results and Validation

In this Chapter we will test our model on a sample scenario. The metric considered will be normalized NLI η (formulas (1.21), (1.22) and (1.31)), which does not depend on signal power.

Test scenario topology can be visualized in Figure 4.1, in which we change accumulating and compensating dispersion values as described in the following, in such a way to evaluate the model from an as general as possible perspective (resulting in multiple scenarios). So, scenarios under test are composed as follows:

- 6 equal spans made of a piece of 50 km LMF with dispersion coefficient D_1 ps/nm/km and EDFA compensating for loss. $D_1 \in$ {-4,-8,-16}.

- 1 final span made of a piece of a piece of DCF with dispersion coefficient D_2 ps/nm/km, in such a way to leave the same inline accumulated dispersion residual of 360 ps/nm. Also in that span we have EDFA compensating for loss. $D_2 \in \{4,8,16\}$.

- Number of loop repetitions N is set to 3, leading to a total of 21 spans.

- All the fibers have a loss coefficient $\alpha = 0.2\ \frac{dB}{km}$ and non-linearity coefficient $\gamma = 0.00127\ \frac{1}{W \cdot km}$

- All the EDFAs work in transparency ($A_i G_i = 1$).

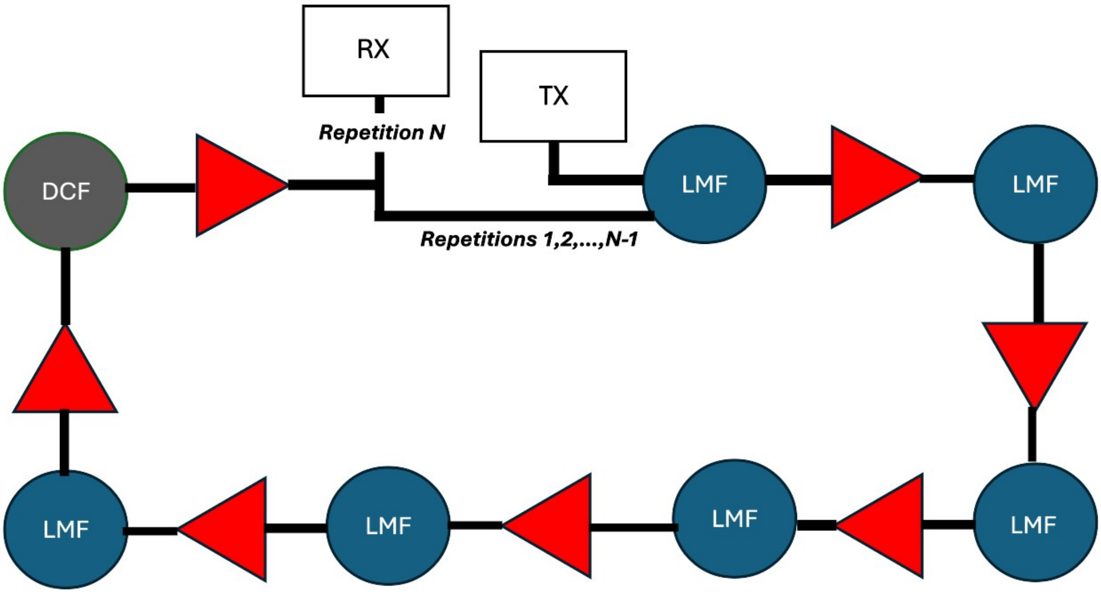

Figure 4.1: Link Topology

So, taking all the possible D_1 and D_2 combinations we have a total of 9 scenarios, as shown in Table 4.1:

D_1 \ D_2	4 ps/nm/km	8 ps/nm/km	16 ps/nm/km
-4 ps/nm/km	$D_1 = -4, D_2 = 4$	$D_1 = -4, D_2 = 8$	$D_1 = -4, D_2 = 16$
-8 ps/nm/km	$D_1 = -8, D_2 = 4$	$D_1 = -8, D_2 = 8$	$D_1 = -8, D_2 = 16$
-16 ps/nm/km	$D_1 = -16, D_2 = 4$	$D_1 = -16, D_2 = 8$	$D_1 = -16, D_2 = 16$

Table 4.1: Scenarios under test

A remarkable observation to be done is the following: since in each of 9 scenarios we leave the same fixed inline residual at the end of the loop and dispersion coefficients values are fixed, the only way we have to control the residual dispersion is to play with DCF length, which values can be found at Table 4.2

Differently from DCUs, DCFs are physical fibers, so together with dispersion compensation, they intrinsecally introduce non-linearity: it will be interesting to see how this impacts on coherency, even if most of DCF fiber length values are much higher than typical values used in real systems.

d_1 \ d_2	4 ps/nm/km	8 ps/nm/km	16 ps/nm/km
-4 ps/nm/km	210 km	105 km	52.5 km
-8 ps/nm/km	510 km	255 km	127.5 km
-16 ps/nm/km	1110 km	555 km	277.5 km

Table 4.2: DCF length

So we can take a look at the accumulated dispersion maps:

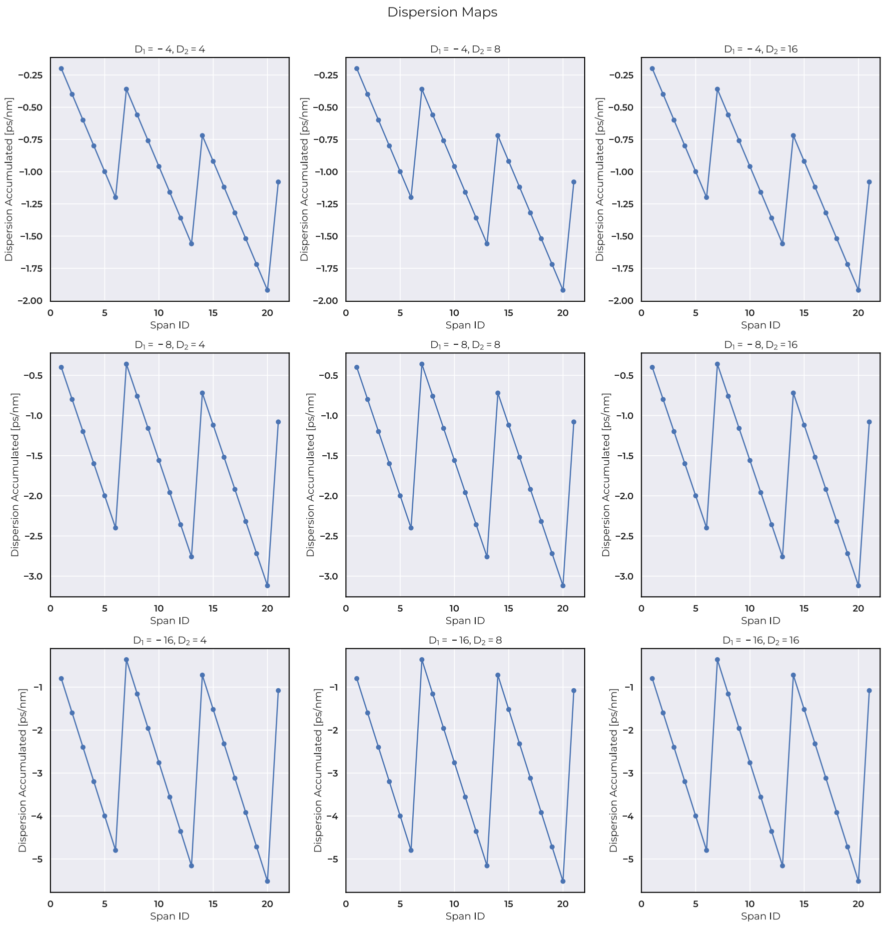

Figure 4.2: Dispersion Maps

Obviously, since in each scenario first 6 spans have an unique D_1 value and we leave fixed inline residual value at the end of each loop, this results in letting

DCF segment introduce the same amount of dispersion for all the cases with equal D_1: so, independently from D_2 value, scenarios with same D_1 present the same dispersion map.

For what concerns signal WDM spectrum, we use the following parameters:

- Number of channels $N_{ch} = 9$
- Symbol Rate $R_s = 63\ Gbaud$
- Channel Spacing $\Delta f = 67\ GHz$
- Modulation Format DP 2-PSK
- Root Raised Cosine shaping filter for each channel

4.1 Spectral Disaggregation

To test that spectral disaggregation is working, we have to verify equation (2.1), so we run simulations with spectral disaggregated strategy as explained in section 3.2.1. In the presented plots we observe first of all the pump and probe disaggregation in Figure 4.3, where

$$\Delta\eta_{SCI,i} = \eta_{SCI,i} - \eta_{SCI,i-1}, \qquad \Delta\eta_{XCI,k,i} = \eta_{XCI,k,i} - \eta_{XCI,k,i-1} \tag{4.1}$$

are shown, where $i \in \{1, 2, \ldots, N_{\text{spans}}\}$. Here we remark that all these values are simulation outputs.

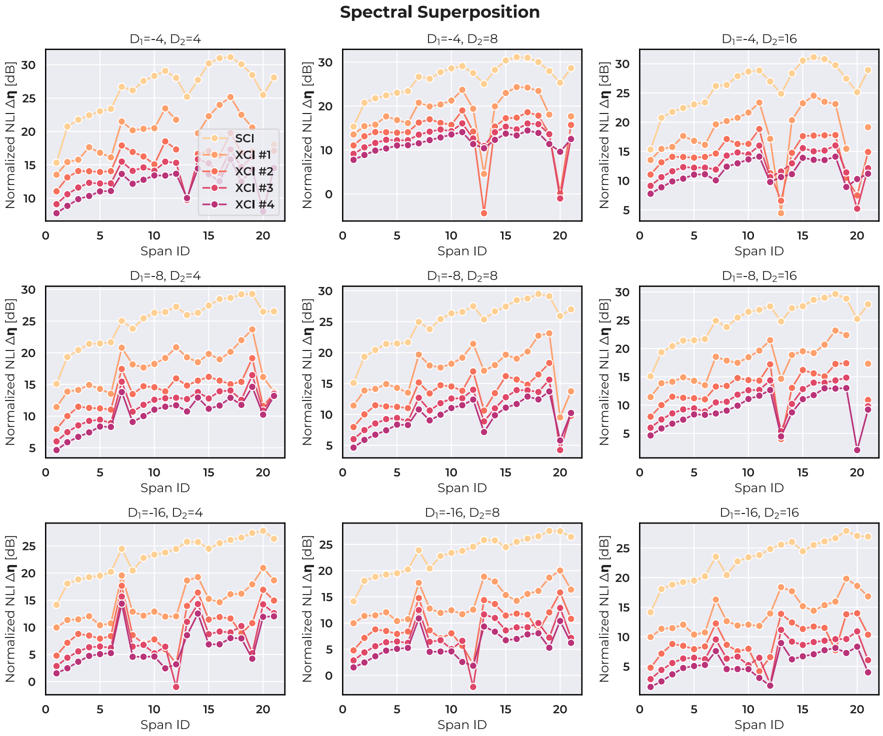

Figure 4.3: Pump and probes spectral disaggregated curves

In Figure 4.4, the red curve represents the superposition of all disaggregated Normalized NLIs seen in Figure 4.3 compared with the Multichannel simulation. The operation performed here is:

$$\Delta\eta_i = \Delta\eta_{SCI,i} + 2\sum_{k=1}^{N_p} \Delta\eta_{XCI,k,i}, \tag{4.2}$$

which holds due to symmetric spectrum.

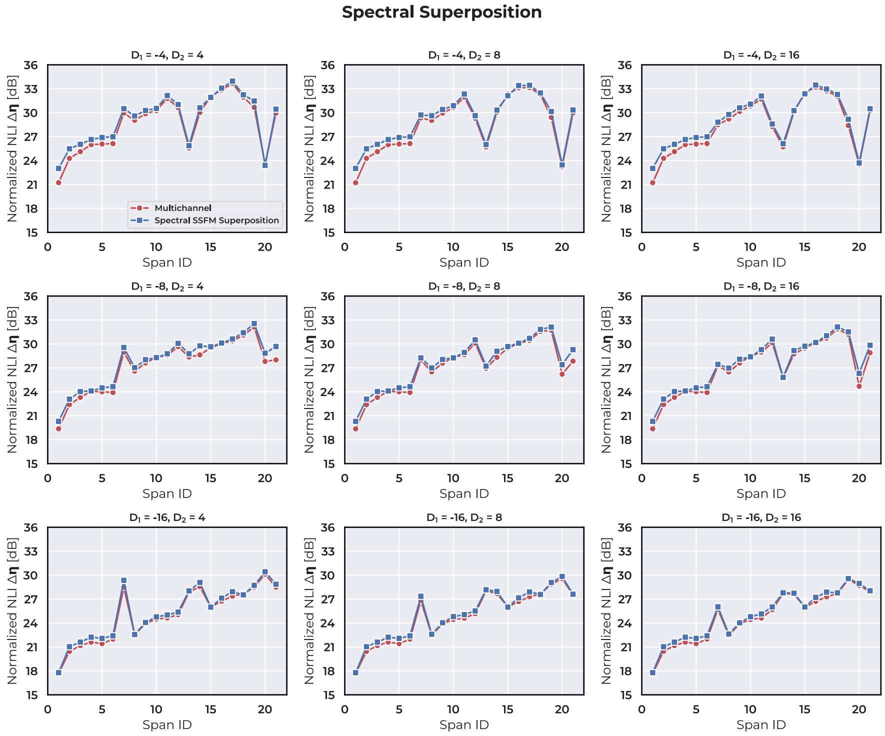

Figure 4.4: Pump and probe superposition vs Multichannel

so we are looking at overall NLI gradient: the behavior of the two curves is pretty similar, but even if this representation is useful to understand how NLI is introduced in each span independently from the other ones, the system actually accumulates these noise contributions, as seen in Figure (2.2). So in order to get the actual noise accumulated, we have to sum cumulatively per span normalized NLIs:

$$\eta_{acc,i} = \sum_{k=1}^{i} \Delta\eta_k \tag{4.3}$$

The resulting curves can be found at Figure 4.5.

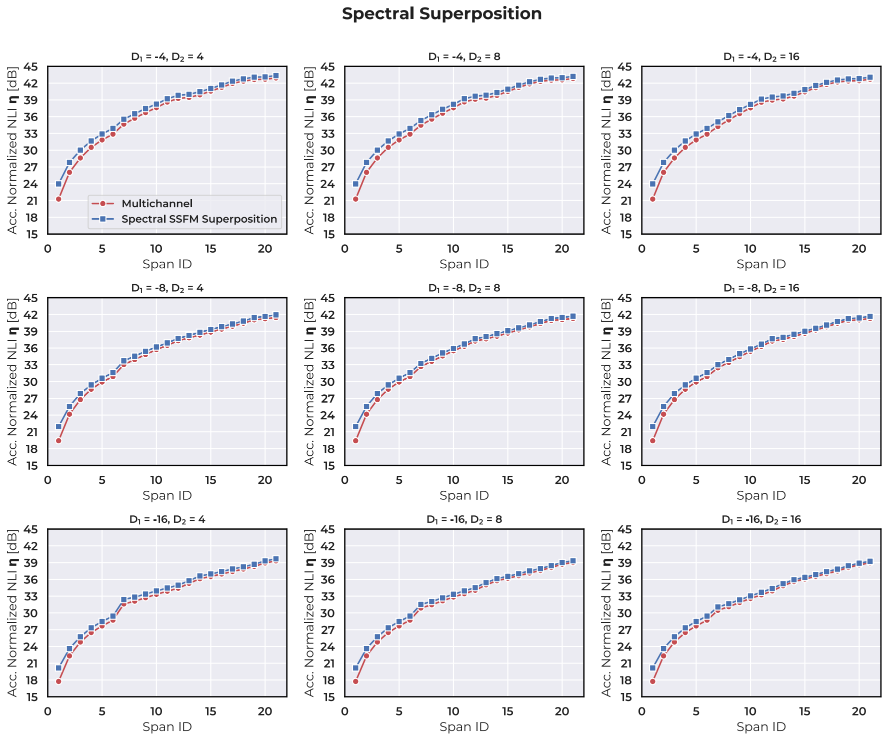

Figure 4.5: Pump and probe accumulated superposition vs Multichannel

Here we observe that superposition of simulated pump and probe disaggregated data overlaps almost perfectly with multichannel data, being a little bit conservative in the initial spans but converging completely at the end of the link. First validation step is so achieved, confirming that full aggregated result is well approximated by spectral disaggregated approach.

However, in this context Kerr Effect is active on all the spans, so we have a spectral disaggregated but spatially aggregated scenario. Next step is so to enter in spatial disaggregation analysis proceeding toward the semi-analitical modeling presented.

4.2 Spatial Disaggregation

With spectral disaggregation we confirmed that full multichannel results can be reconstructed by relying just on each pump SCI/XCI contribution. In spatial disaggregation we go deeper analyzing each span NLI, testing the disaggregation formula (2.3) works properly, evaluating how much GN model estimation for NLI and ML one for C_{ij} are accurate. Since we use normalized NLI as metric, formula

(2.3) translates in:

$$\Delta\eta_{XCI,k,i} = \Delta\eta_{XCI,pure,k,i} + 2\sum_{j=1}^{i-1} C_{k,ij}\sqrt{\Delta\eta_{XCI,pure,k,i}\Delta\eta_{XCI,pure,k,j}} \tag{4.4}$$

Remarking, from a notation point of view, that $k = 0$ corresponds to SCI.

First of all, we assess the pure contributions $\Delta\eta_{XCI,pure,k,i}$, comparing their GN Model estimation with ground truth pump and probe curves, both coherent and incoherent ones. So we plot:

- Green curve with markers, that represents pure NLI contributions per span, extracted from simulations (spatially disaggregated ones where Kerr-effect is turned on only on span i)
- Green curve without markers, that represents pure NLI contributions computed with GN model
- Red curve that represents ground truth pump and probe propagation, i.e. data from a simulation where Kerr-effect is active in all the spans

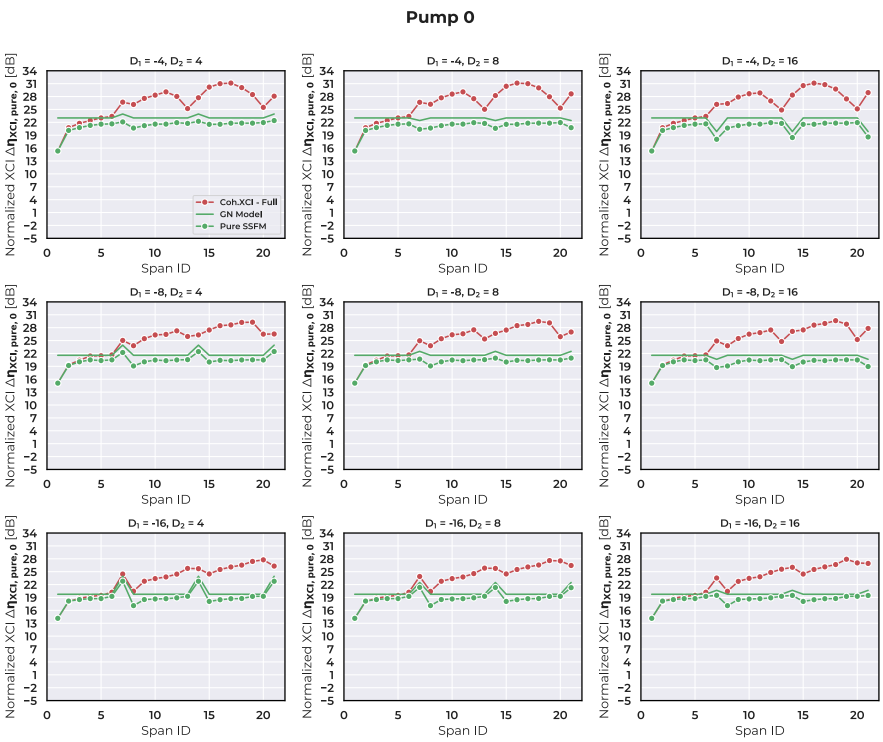

Pump 1

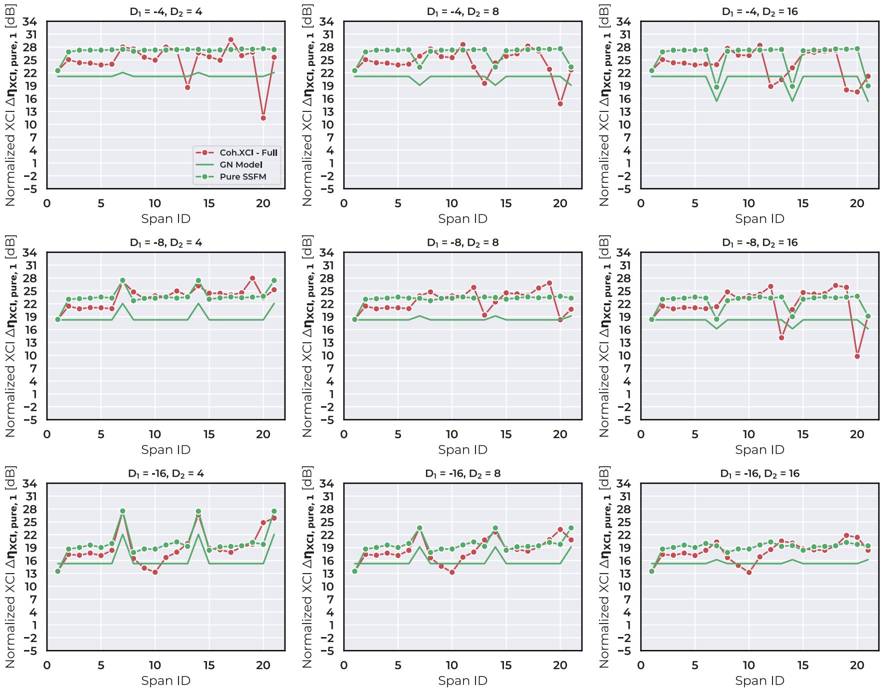

D₁ = -4, D₂ = 4
D₁ = -4, D₂ = 8
D₁ = -4, D₂ = 16
D₁ = -8, D₂ = 4
D₁ = -8, D₂ = 8
D₁ = -8, D₂ = 16
D₁ = -16, D₂ = 4
D₁ = -16, D₂ = 8
D₁ = -16, D₂ = 16
Coh.XCI - Full
GN Model
Pure SSFM
Normalized XCI $\Delta\eta_{XCI,\,pure,\,1}$ [dB]
Span ID

Pump 2

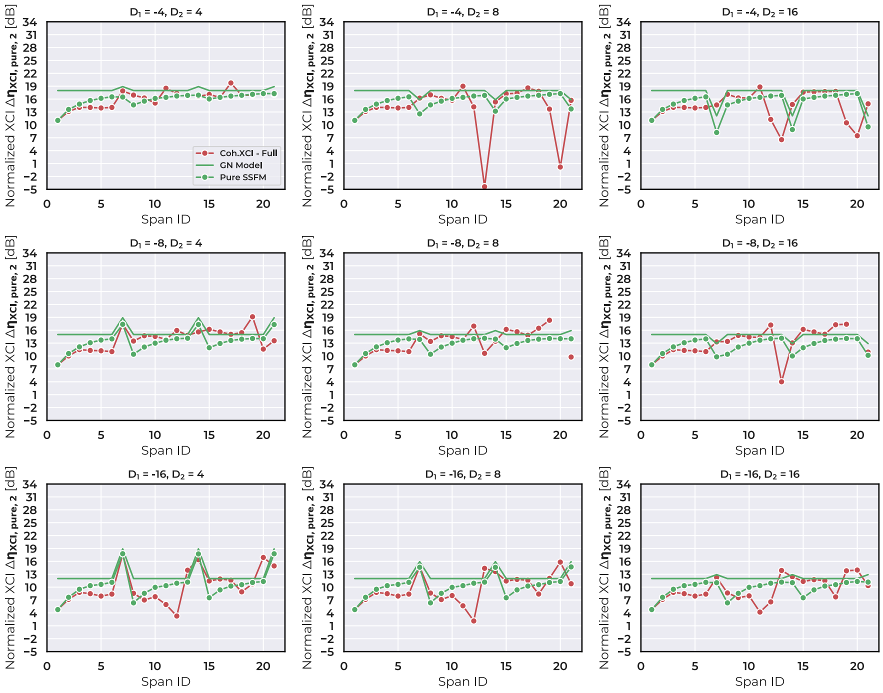

D₁ = -4, D₂ = 4
D₁ = -4, D₂ = 8
D₁ = -4, D₂ = 16
D₁ = -8, D₂ = 4
D₁ = -8, D₂ = 8
D₁ = -8, D₂ = 16
D₁ = -16, D₂ = 4
D₁ = -16, D₂ = 8
D₁ = -16, D₂ = 16
Coh.XCI - Full
GN Model
Pure SSFM
Normalized XCI $\Delta\eta_{XCI,\,pure,\,2}$ [dB]
Span ID

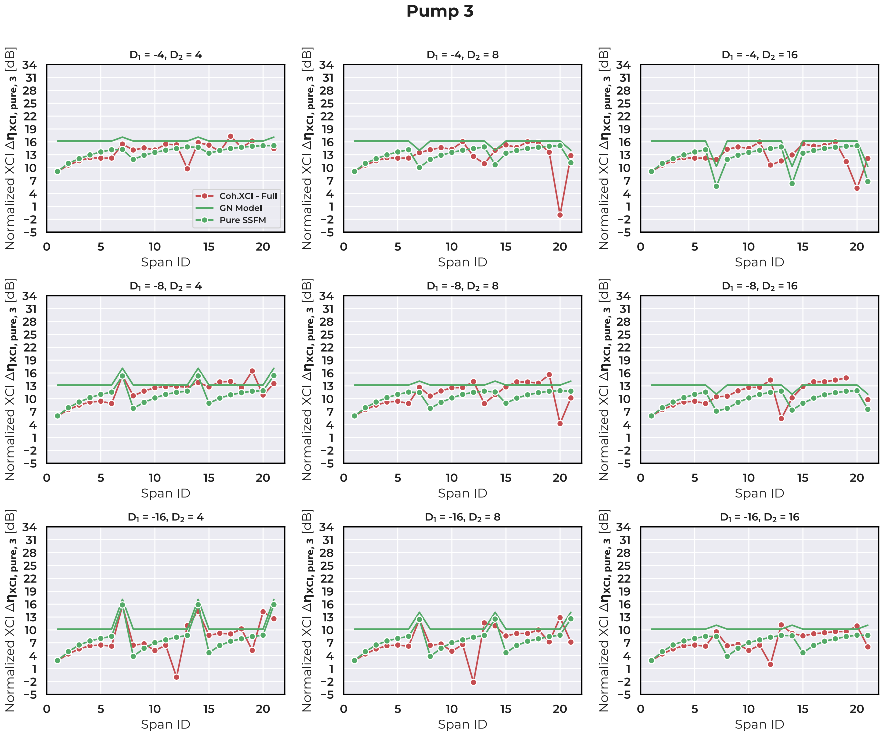
Pump 3
D_1 = -4, D_2 = 4
D_1 = -4, D_2 = 8
D_1 = -4, D_2 = 16
D_1 = -8, D_2 = 4
D_1 = -8, D_2 = 8
D_1 = -8, D_2 = 16
D_1 = -16, D_2 = 4
D_1 = -16, D_2 = 8
D_1 = -16, D_2 = 16
Normalized XCI $\Delta\eta_{XCI, pure, 3}$ [dB]
Span ID
Coh.XCI - Full
GN Model
Pure SSFM

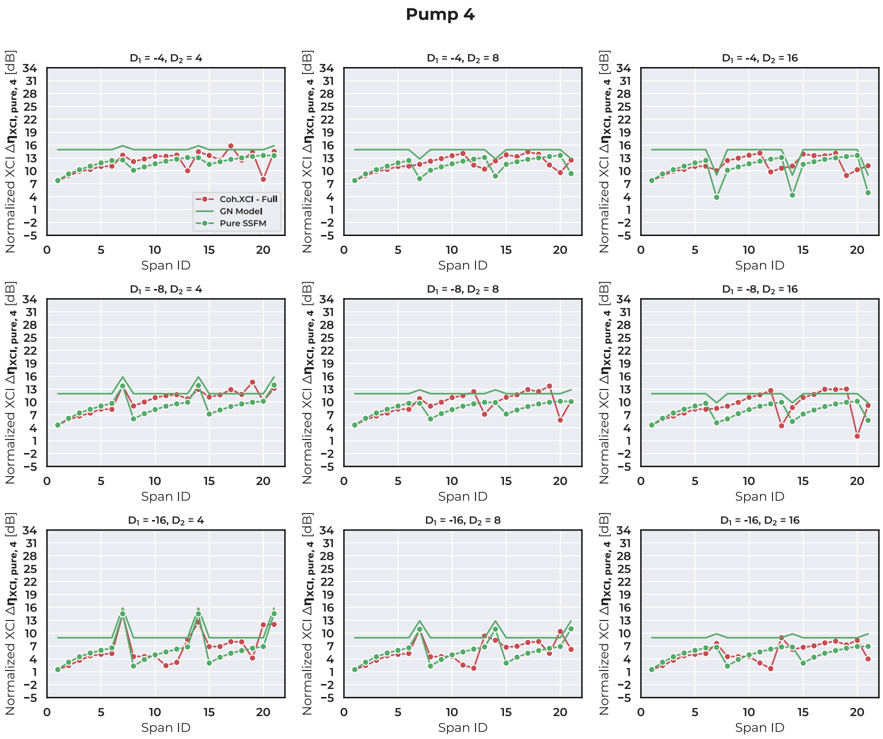
Pump 4
D_1 = -4, D_2 = 4
D_1 = -4, D_2 = 8
D_1 = -4, D_2 = 16
D_1 = -8, D_2 = 4
D_1 = -8, D_2 = 8
D_1 = -8, D_2 = 16
D_1 = -16, D_2 = 4
D_1 = -16, D_2 = 8
D_1 = -16, D_2 = 16
Normalized XCI $\Delta\eta_{XCI, pure, 4}$ [dB]
Span ID
Coh.XCI - Full
GN Model
Pure SSFM

As expected, NLI description based only on pure contributions is not sufficient to address correctly the problem, since neither of the two green curves matches with the red one. Going into the details of pure NLI estimation, as seen in section 1.2.4, GN model should in every case overestimate the actual $\Delta\eta$ values due to gaussianization hypothesis, and this is confirmed for all the pumps except for pump 1, for which a little bit more attention is required: here we are observing not only the NLI noise but also another noise contribution together with it, that after further investigations, resulted to be linear crosstalk introduced by Spectral Broadening.

4.2.1 Pump 1 case: Spectral Broadening

Spectral broadening is a phenomenon caused by tight channel spacing between pump and probe and way lower probe power with respect the pump one. The observed effect is introduced by SCI and creates new, unwanted frequencies outside pump bandwidth in a four wave mixing-like crosstalk, generating so additive noise over NLI. In any case, Spectral Broadening comes out just as artifact of our method used to estimate XCI by simulations consisting in setting the probe very low in power with respect the pump. So Spectral Broadening will be totally negligible in the actual scenario with a set of multiple channels at the same launch power, but we have anyway to deal with it to provide an overall disaggregated NLI estimation.

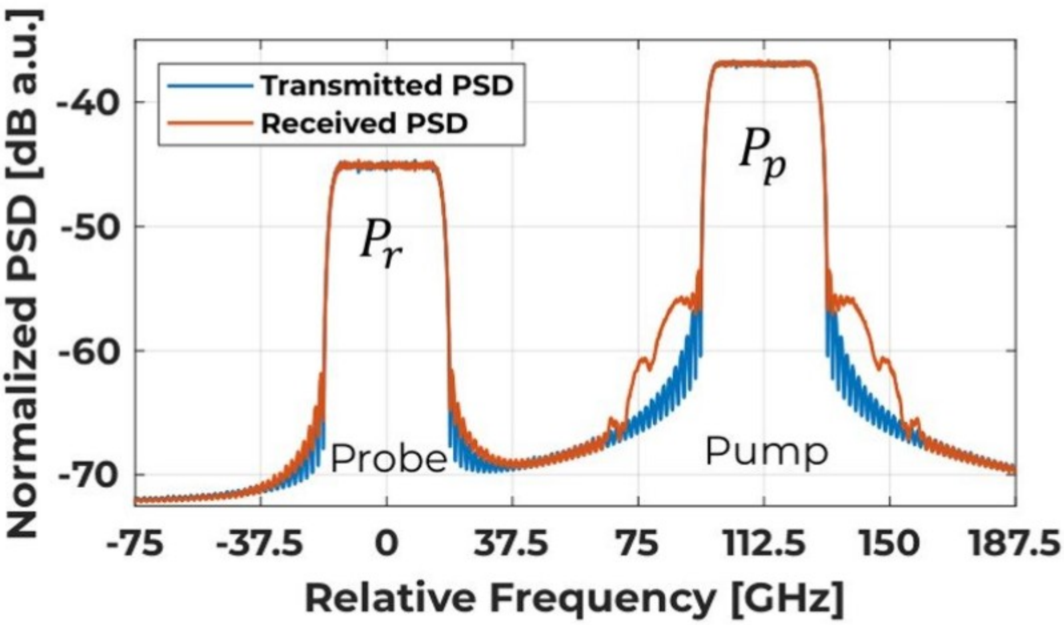

Figure 4.6: Spectral Broadening example in a pump and probe scenario

In order to clean simulated values from Spectral Broadening, we developed a proper algorithm starting from the equations:

$$P_{N,1} = P_{probe,1} P_{pump}^2 \eta_{\mathrm{XCI}} + P_{pump}^3 k_{\mathrm{SBXT}}$$

$$P_{N,2} = P_{probe,2} P_{pump}^2 \eta_{\mathrm{XCI}} + P_{pump}^3 k_{\mathrm{SBXT}} \tag{4.5}$$

That represent two different NLI powers taken at different probe powers, taking into account the linear crosstalk contribution with the term $P_{pump}^3 k_{\mathrm{SBXT}}$.

The linear system solutions are:

$$\eta_{\mathrm{XCI}} = \frac{P_{N,2} - P_{N,1}}{P_{pump}^2 \left(P_{probe,2} - P_{probe,1}\right)}$$

$$k_{\mathrm{SBXT}} = \frac{P_{N,1} P_{probe,2} - P_{N,2} P_{probe,1}}{P_{pump}^3 \left(P_{probe,2} - P_{probe,1}\right)} \tag{4.6}$$

So we clean η_{XCI} as follows:

$$\eta_{XCI,cleaned} = \eta_{XCI,not\_cleaned} - \frac{P_{pump}}{P_{probe}} k_{SBXT} \tag{4.7}$$

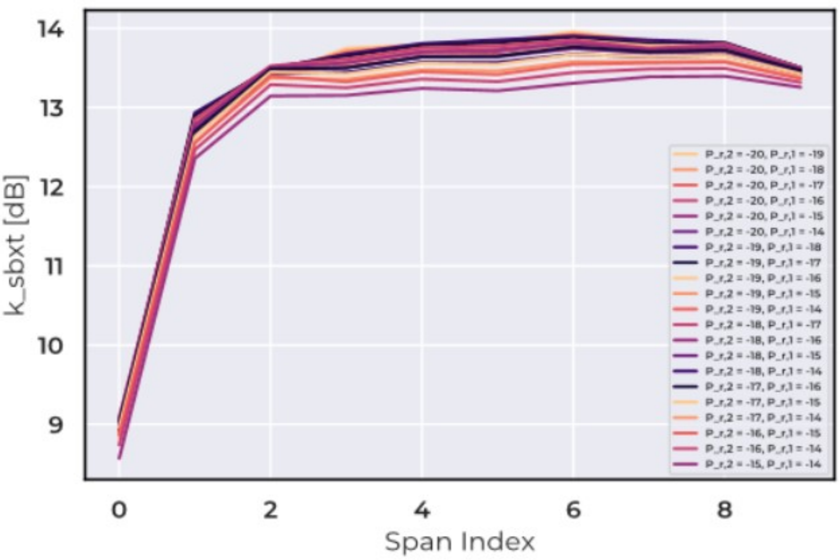

Figure 4.7: k_{SBXT} computed for different couples of probe power values

Theoretically, since the phenomenon is linear, k_{SBXT} should be equal independently from the power couples taken into account. Actually we test it anyway for all probe power couples in the set of values [-20, -19, -18, -17, -16, -15, -14] dBm, and we can observe the result in Figure 4.7. As expected, k_{SBXT} presents very little fluctuations depending on the power pair used, so in order to clean pump 1 XCI from spectral broadening, we just need to run two different simulations at two different probe powers: we usually already have the ones used with probe power set to -18 dBm, so it's sufficient to run another set of spatial disaggregated simulation with a different probe power. We have chosen -14 dBm as probe power value for such simulations.

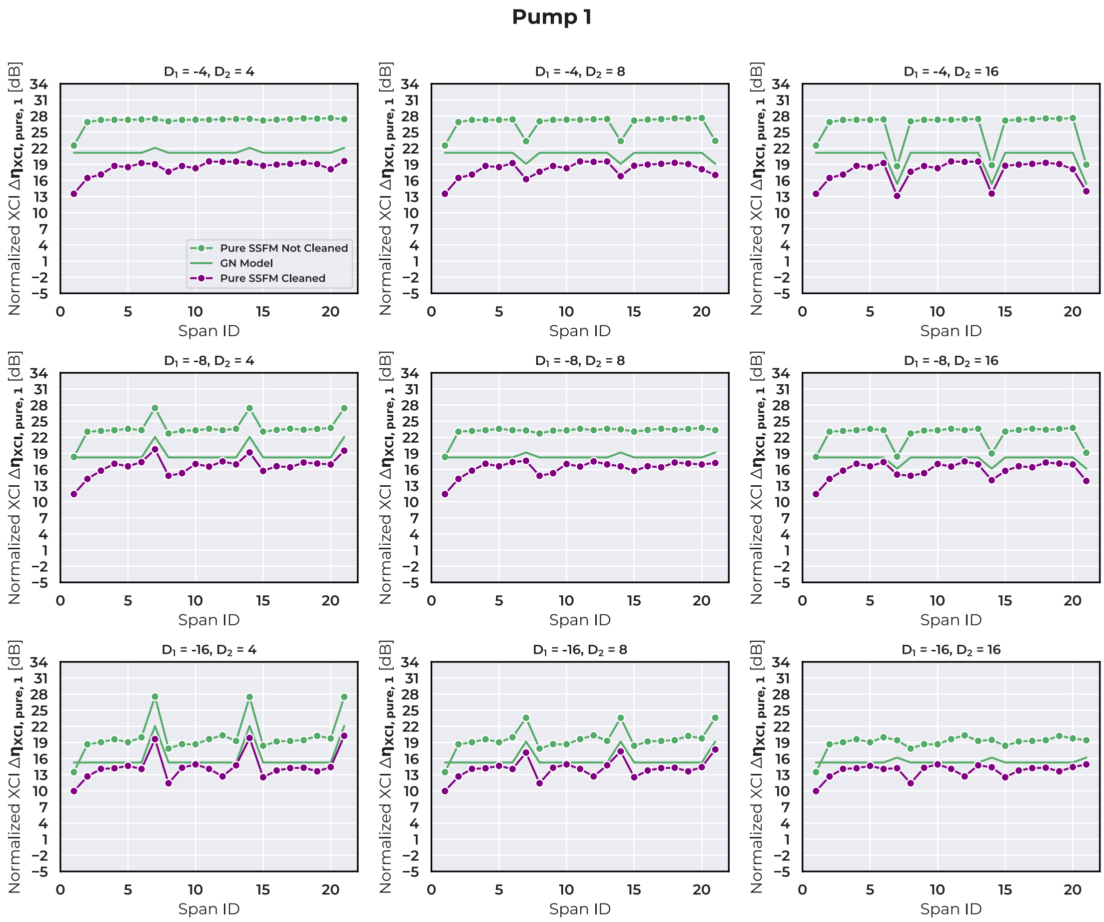

Figure 4.8: Pump 1 cleaned from spectral broadening

After correction is applied, we can see results in 4.8, where analytical GN model is above the simulated pure cleaned NLI (purple curve) in all the plots, so it's consistent with the theory.

Once understood how to address the pure contrinutions, we can move forward to evaluate coherency contributions to estimate the actual NLI along the link.

So in the following plots will be displayed:

- Red curve as pump and probe ground truth
- Blue curve as result of ΔP formula (2.16), where both pure contributions and correlation coefficients are extracted from simulations. So this represents spatial disaggregation ground truth
- Grey curve that represents ΔP computed with $\Delta\eta_{XCI,pure,k,i}$ and $\Delta\eta_{XCI,pure,k,j}$ estimated through GN Model and C_{ij} taken from simulations
- Black curve that is obtained with ΔP formula where $\Delta\eta_{XCI,pure,k,i}$ and $\Delta\eta_{XCI,pure,k,j}$ are computed with GN Model and C_{ij} are estimated with Machine Learning.

  As for spectral disaggregation, we will plot both NLI gradient and accumulated, due to considerations done previously.

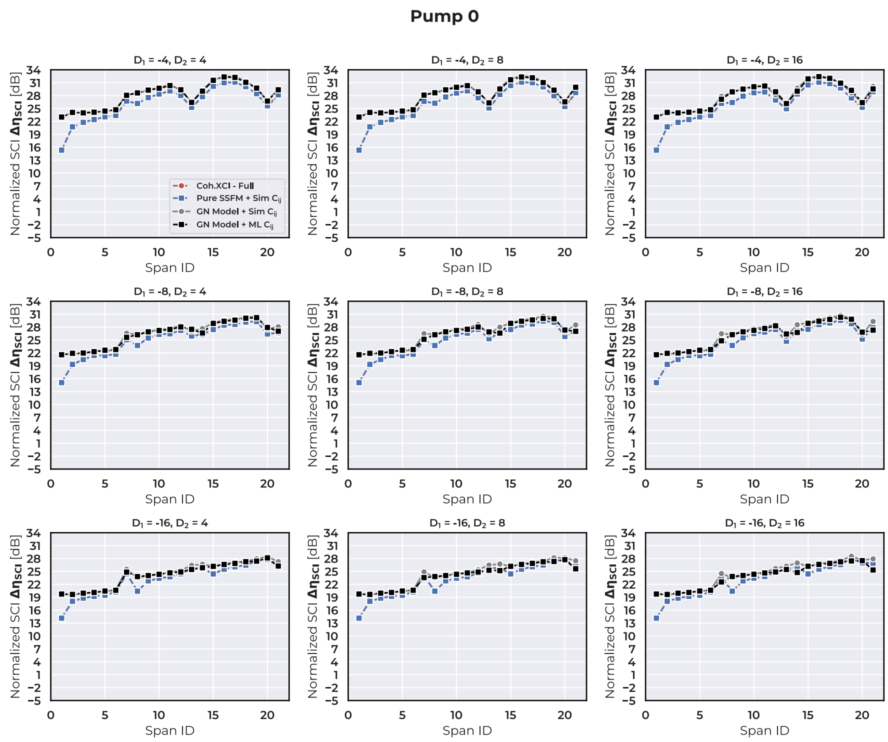

Pump 1

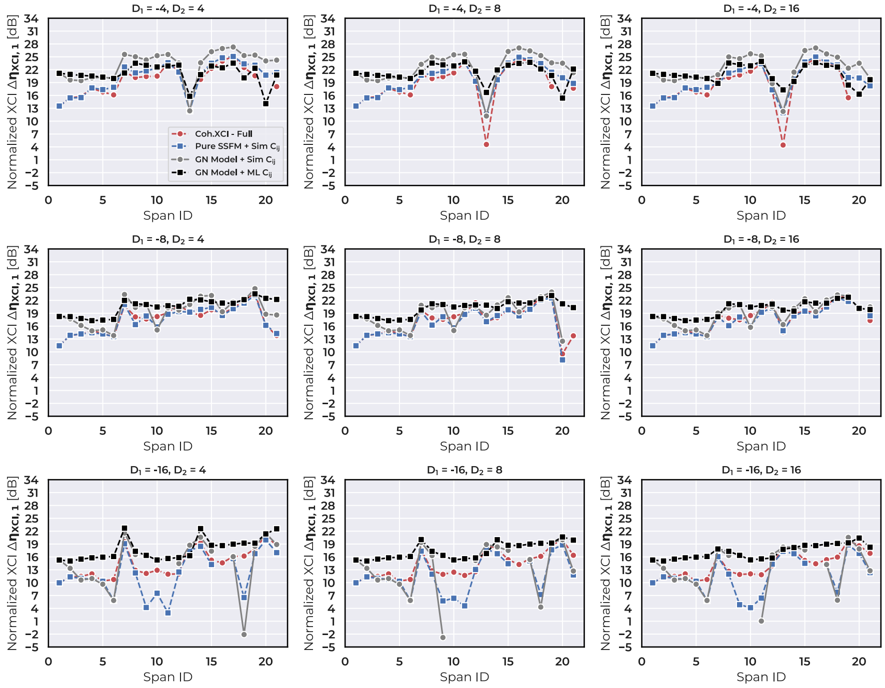
D1 = -4, D2 = 4
D1 = -4, D2 = 8
D1 = -4, D2 = 16
D1 = -8, D2 = 4
D1 = -8, D2 = 8
D1 = -8, D2 = 16
D1 = -16, D2 = 4
D1 = -16, D2 = 8
D1 = -16, D2 = 16
Normalized XCI Δηxci, 1 [dB]
Span ID
Coh.XCI - Full
Pure SSFM + Sim Cij
GN Model + Sim Cij
GN Model + ML Cij

Pump 2

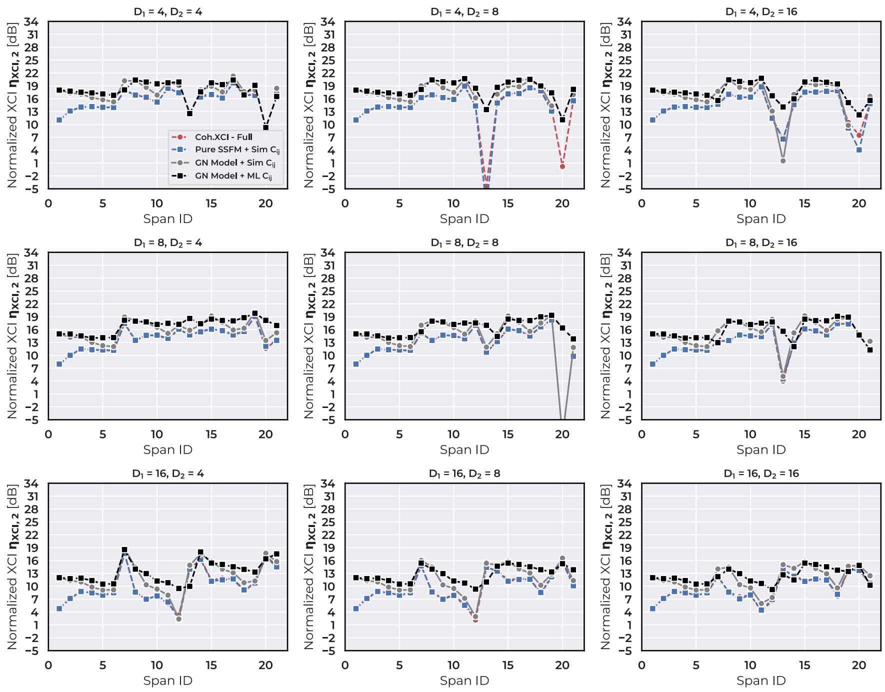
D1 = 4, D2 = 4
D1 = 4, D2 = 8
D1 = 4, D2 = 16
D1 = 8, D2 = 4
D1 = 8, D2 = 8
D1 = 8, D2 = 16
D1 = 16, D2 = 4
D1 = 16, D2 = 8
D1 = 16, D2 = 16
Normalized XCI ηxci, 2 [dB]
Span ID
Coh.XCI - Full
Pure SSFM + Sim Cij
GN Model + Sim Cij
GN Model + ML Cij

Pump 3

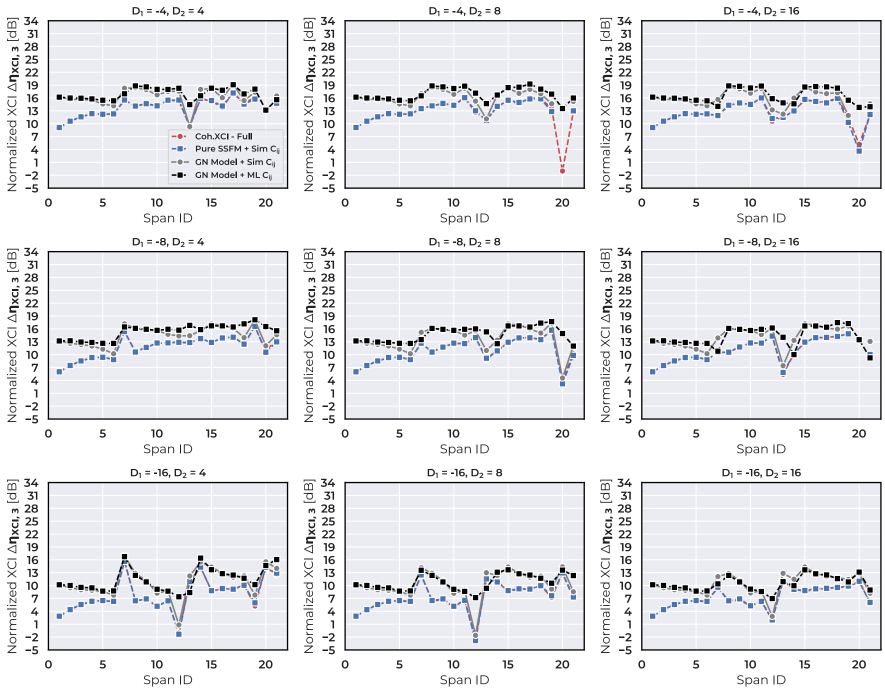
D1 = -4, D2 = 4
D1 = -4, D2 = 8
D1 = -4, D2 = 16
D1 = -8, D2 = 4
D1 = -8, D2 = 8
D1 = -8, D2 = 16
D1 = -16, D2 = 4
D1 = -16, D2 = 8
D1 = -16, D2 = 16
Normalized XCI Δηxci, 3 [dB]
Span ID
Coh.XCI - Full
Pure SSFM + Sim Cij
GN Model + Sim Cij
GN Model + ML Cij

Pump 4

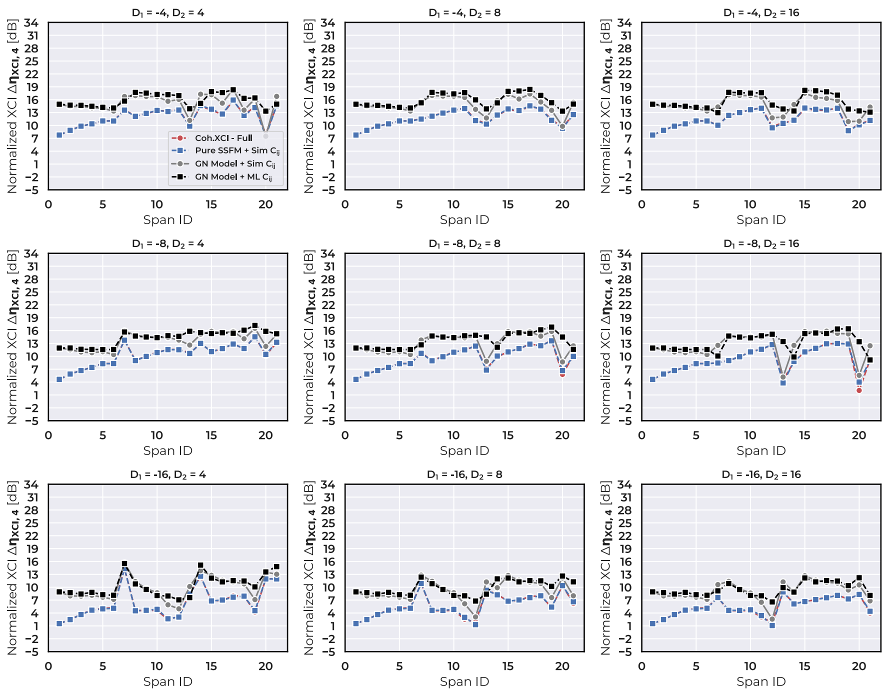
D1 = -4, D2 = 4
D1 = -4, D2 = 8
D1 = -4, D2 = 16
D1 = -8, D2 = 4
D1 = -8, D2 = 8
D1 = -8, D2 = 16
D1 = -16, D2 = 4
D1 = -16, D2 = 8
D1 = -16, D2 = 16
Normalized XCI Δηxci, 4 [dB]
Span ID
Coh.XCI - Full
Pure SSFM + Sim Cij
GN Model + Sim Cij
GN Model + ML Cij

Pump 0

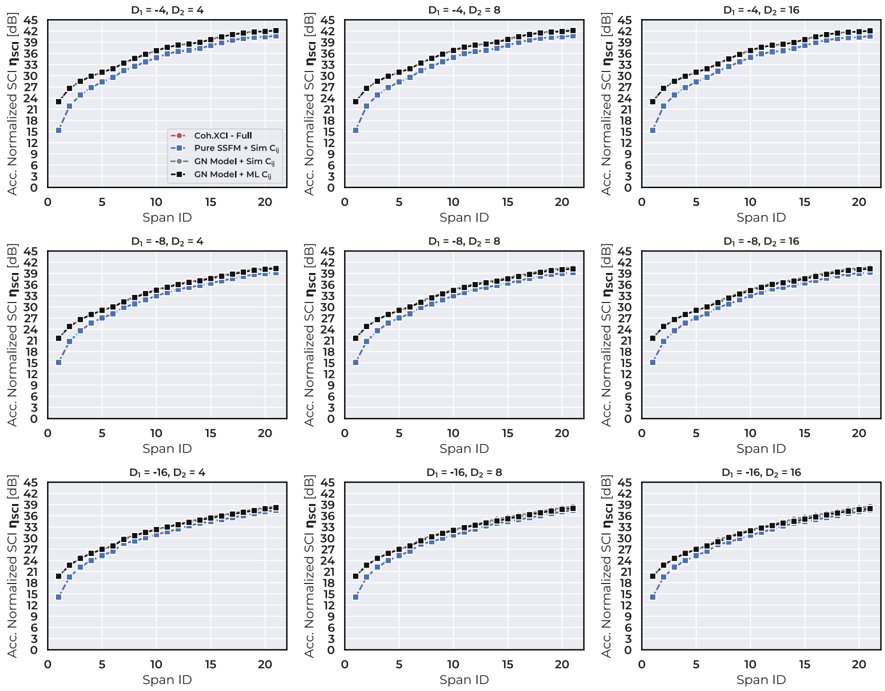
D₁ = -4, D₂ = 4
D₁ = -4, D₂ = 8
D₁ = -4, D₂ = 16
D₁ = -8, D₂ = 4
D₁ = -8, D₂ = 8
D₁ = -8, D₂ = 16
D₁ = -16, D₂ = 4
D₁ = -16, D₂ = 8
D₁ = -16, D₂ = 16
Acc. Normalized SCI ηSCI [dB]
Span ID
Coh.XCI - Full
Pure SSFM + Sim Cij
GN Model + Sim Cij
GN Model + ML Cij

Pump 1

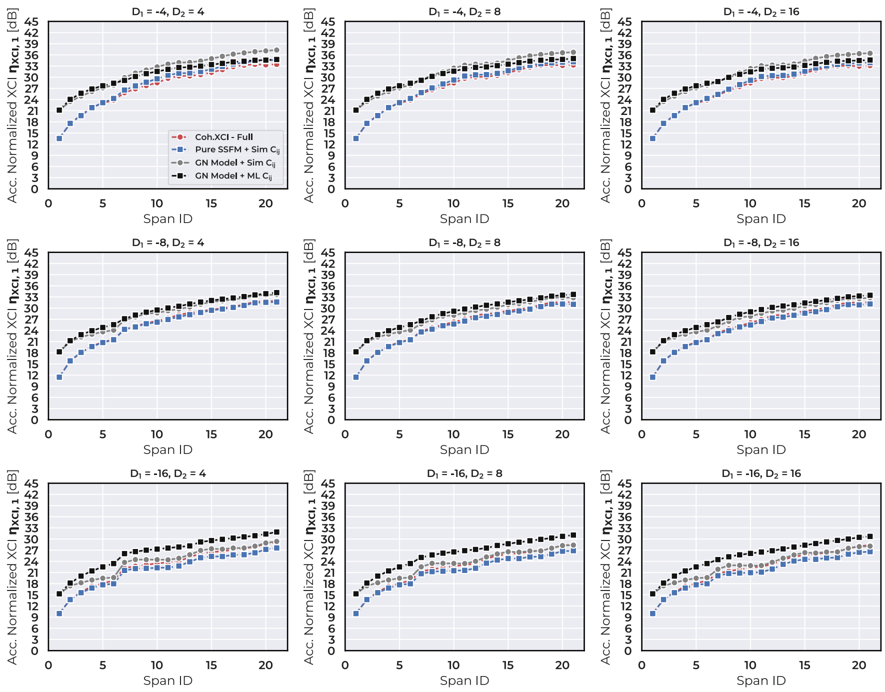
D₁ = -4, D₂ = 4
D₁ = -4, D₂ = 8
D₁ = -4, D₂ = 16
D₁ = -8, D₂ = 4
D₁ = -8, D₂ = 8
D₁ = -8, D₂ = 16
D₁ = -16, D₂ = 4
D₁ = -16, D₂ = 8
D₁ = -16, D₂ = 16
Acc. Normalized XCI ηXCI,1 [dB]
Span ID
Coh.XCI - Full
Pure SSFM + Sim Cij
GN Model + Sim Cij
GN Model + ML Cij

Pump 2

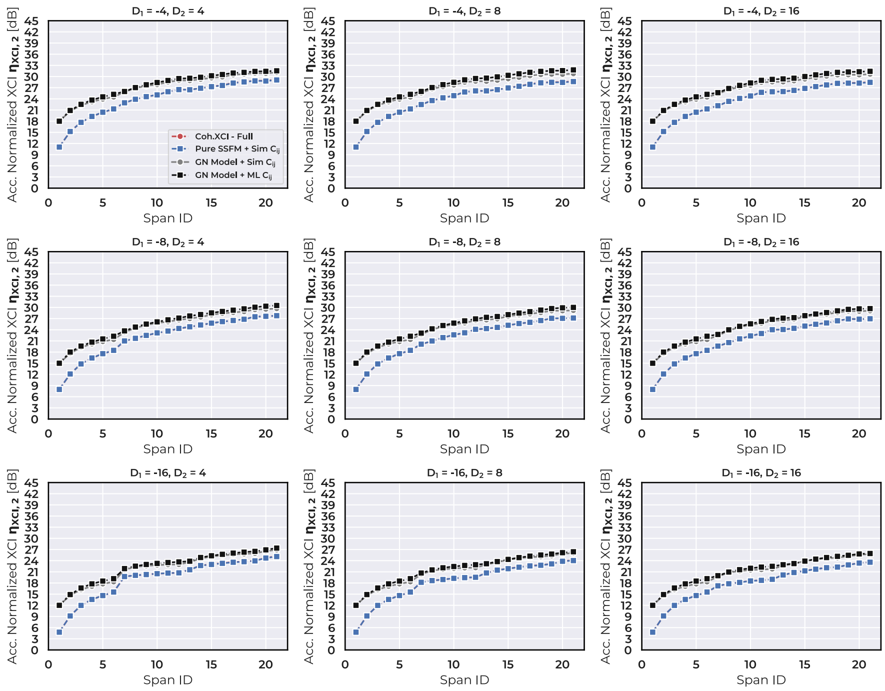
D1 = -4, D2 = 4
D1 = -4, D2 = 8
D1 = -4, D2 = 16
D1 = -8, D2 = 4
D1 = -8, D2 = 8
D1 = -8, D2 = 16
D1 = -16, D2 = 4
D1 = -16, D2 = 8
D1 = -16, D2 = 16
Acc. Normalized XCI ηXCI, 2 [dB]
Span ID
Coh.XCI - Full
Pure SSFM + Sim Cij
GN Model + Sim Cij
GN Model + ML Cij

Pump 3

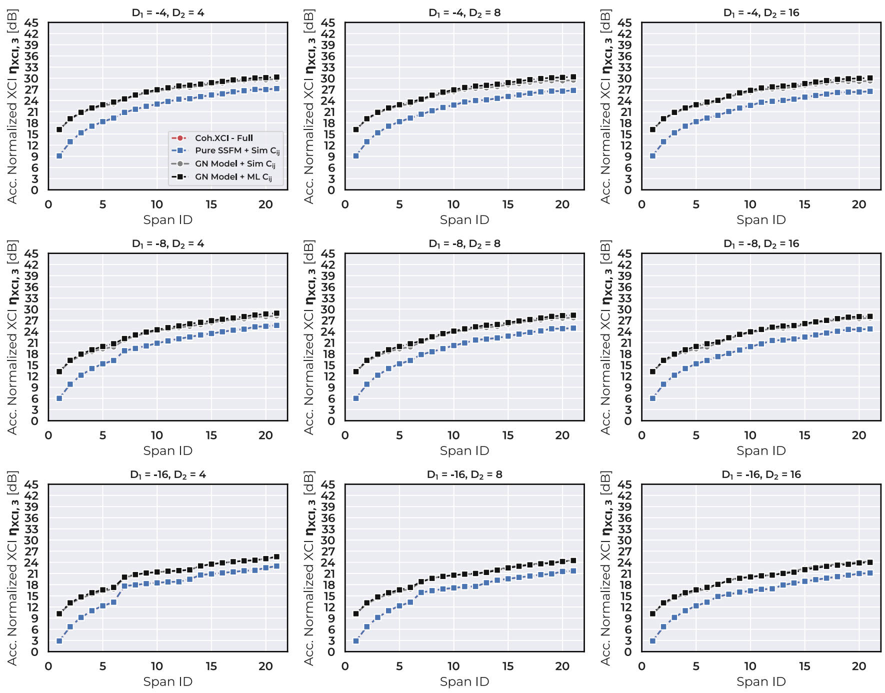
D1 = -4, D2 = 4
D1 = -4, D2 = 8
D1 = -4, D2 = 16
D1 = -8, D2 = 4
D1 = -8, D2 = 8
D1 = -8, D2 = 16
D1 = -16, D2 = 4
D1 = -16, D2 = 8
D1 = -16, D2 = 16
Acc. Normalized XCI ηXCI, 3 [dB]
Span ID
Coh.XCI - Full
Pure SSFM + Sim Cij
GN Model + Sim Cij
GN Model + ML Cij

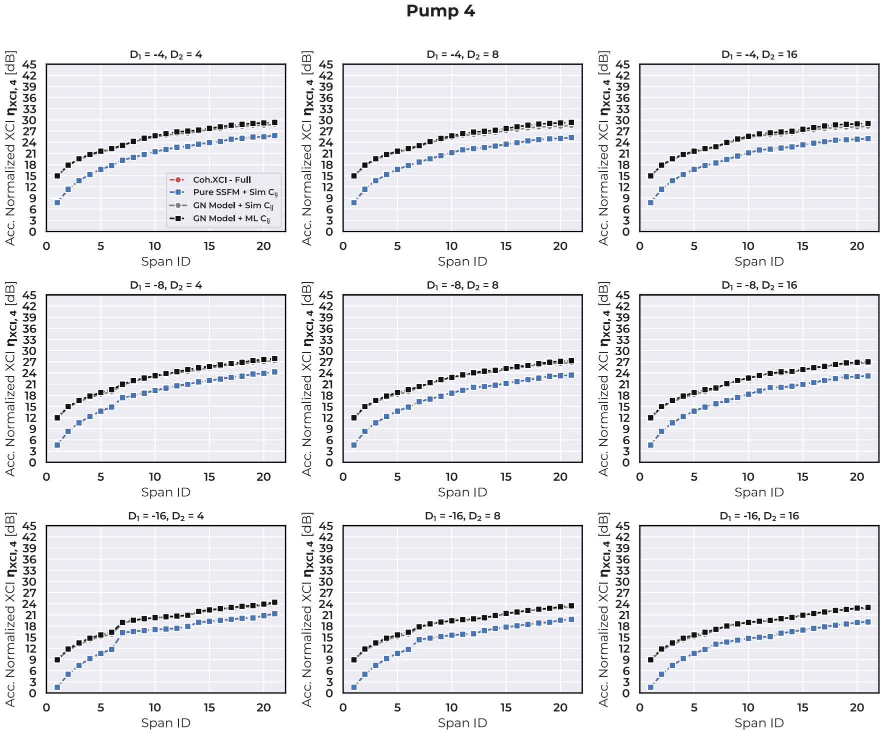

Several considerations can be made on these results: first of all, red curve overlaps perfectly with blue one, confirming that from the theoretical point of view spatial disaggregation model works. For what concerns the analytical estimation, we observe that grey and black curves are mostly overlapped, meaning that correlation coefficients ML estimation is pretty near to the actual values: this will be shown deeper in the next section. In general black/grey curves are more conservative with respect red/blue ones: this is expected, since this gap is due to the already discussed gaussianization hypothesis on pure contributions estimation, which final impact is, as in UT systems, a worst case assessment of the actual NLI figure. What reported in these final comments is true for all the pumps in all scenarios except for pump 1: here the mentioned curves do not overlap perfectly as in other pumps due to spectral broadening, resulting in inaccurate values simulated correlation coefficients: even if we clean SSFM pure values from spectral broadening with the procedure reported above (and the curves displayed actually are), the problem persists. In any case, grey and black curves are still conservative with respect red one in accumulated NLI plots, so that issue does not compromise correct functioning of the model itself.

4.2.2 Correlation Coefficients Analysis

We have shown that the coherent accumulation of the SCI/XCI can be properly addressed with the previously shown model. The model is based on the estimation of the pure terms, intrinsic of each fiber span, which can be conservatively estimated using the incoherent GN Model, and on the estimation of the correlation coefficients between each span couple (i,j), $i > j$. Hence, it is worth to take a look at how the correlation coefficients scale with respect to the considered span couple i,j. Indeed, the pure noise terms of two spans i and j are more and more decorrelated as larger is the chromatic dispersion accumulated between them. Anyway, stated several times, our final semi-analytical model will rely on Machine Learning-predicted C_{ij}, so it's important to check the accuracy of this approach as a further validation, even if in previous section we observed that NLI reconstruction using ML C_{ij} works pretty well. So now we will take a look to correlation coefficients heatmaps for all the spans combinations in all scenarios pump by pump, plotting three different bunches of graphs consisting in:

- Simulated C_{ij}, ground truth from simulations
- Machine Learning predicted C_{ij}
- Absolute error between simulated and ML predictions $|C_{ij,SIM} - C_{ij,ML}|$

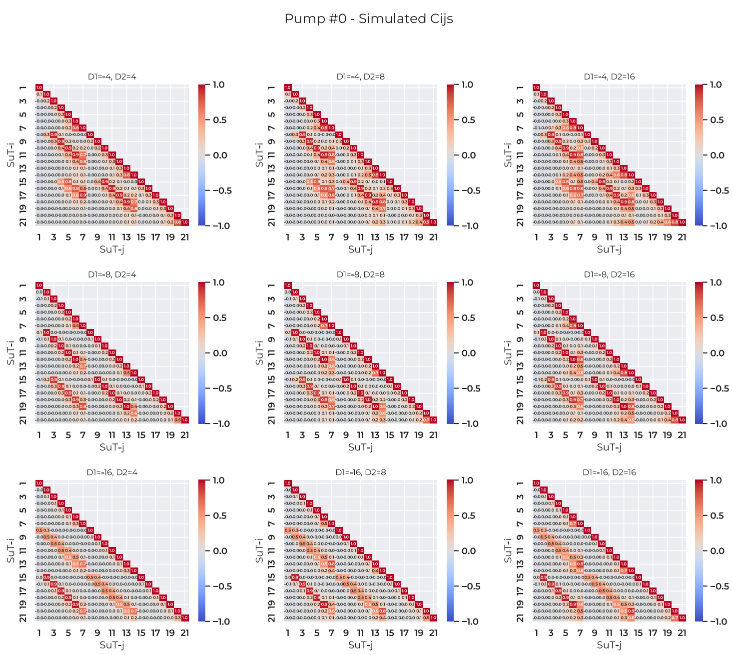

Pump 0 - Machine Learning Cijs

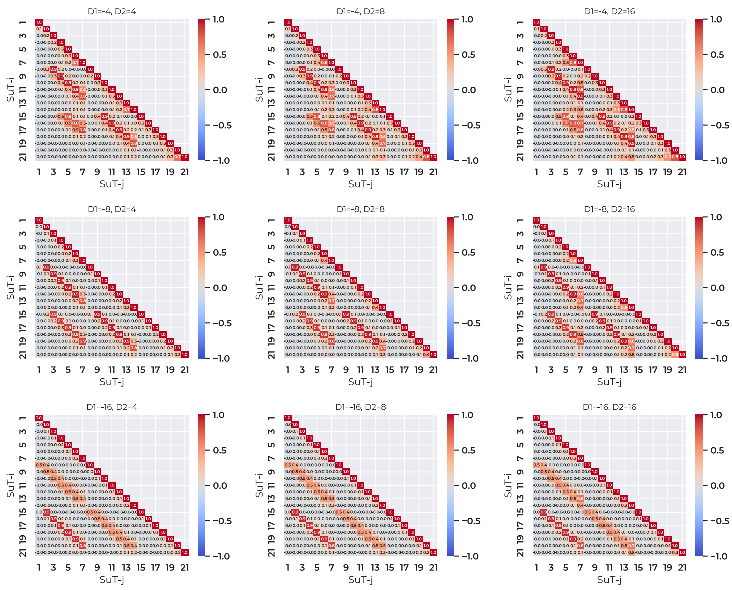

Pump 0 - Absolute Error

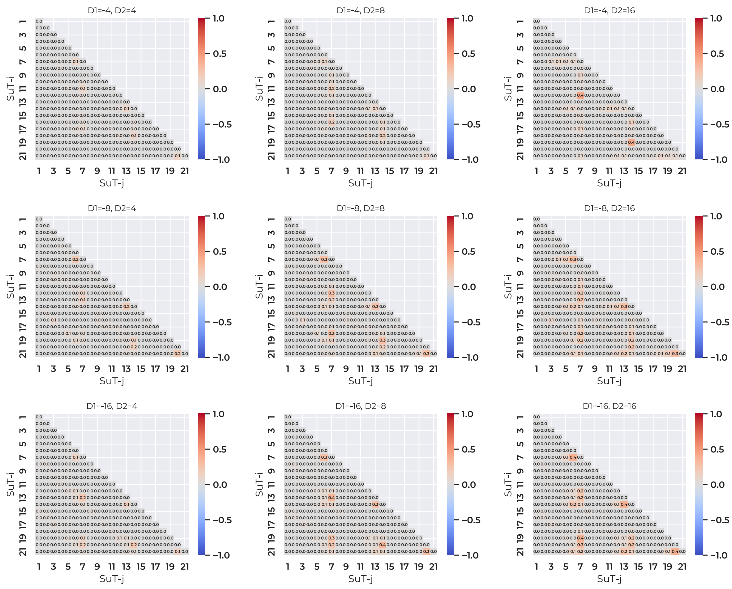

Pump #1 - Simulated Cijs

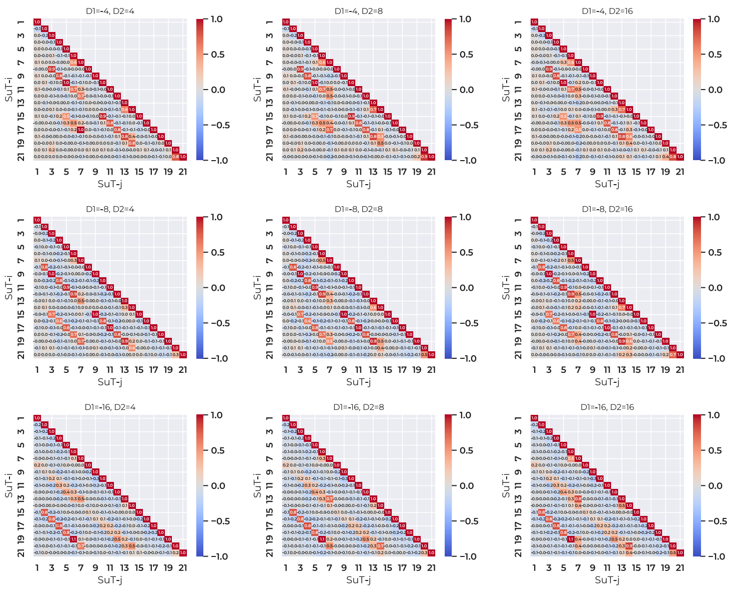

Pump 1 - Machine Learning Cijs

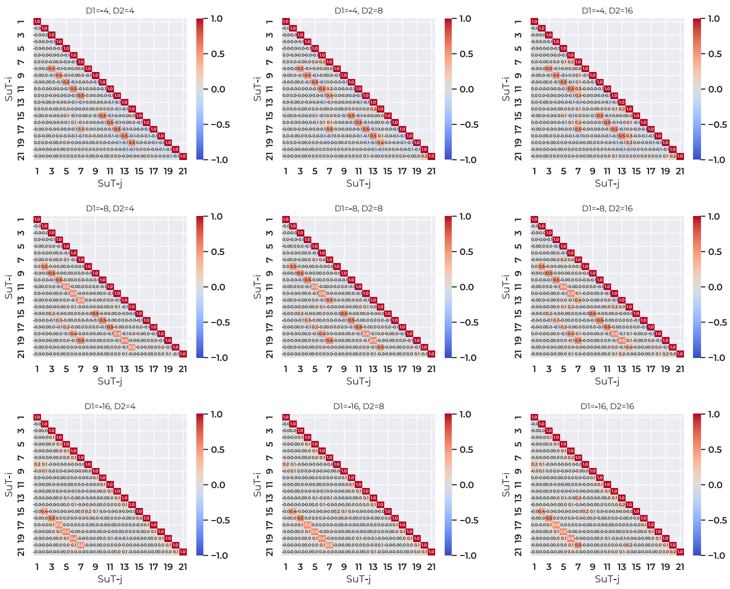

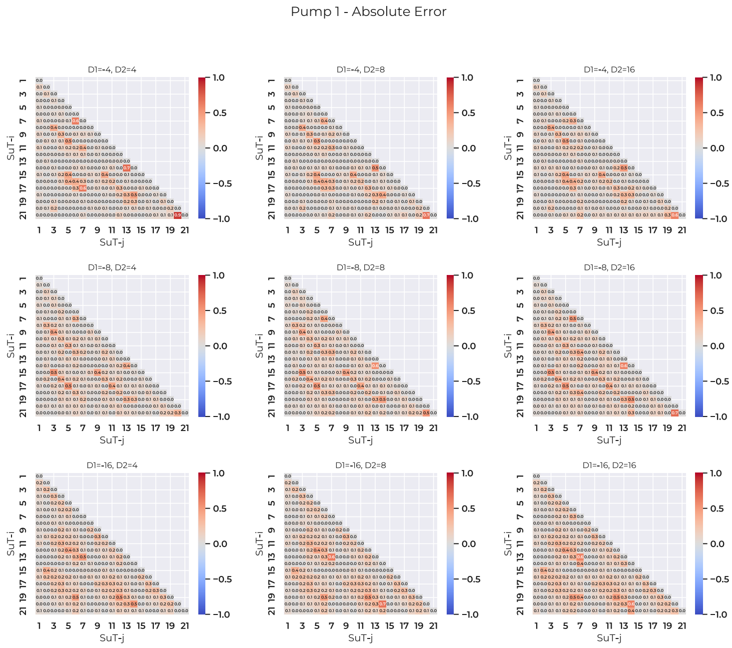
Pump 1 - Absolute Error
D1=-4, D2=4
D1=-4, D2=8
D1=-4, D2=16
D1=-8, D2=4
D1=-8, D2=8
D1=-8, D2=16
D1=-16, D2=4
D1=-16, D2=8
D1=-16, D2=16
SuT-i
SuT-j

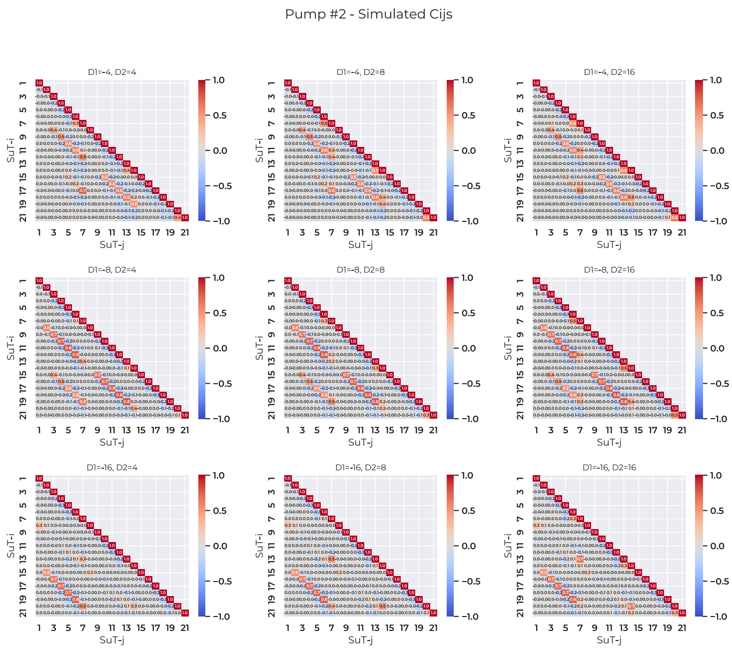
Pump #2 - Simulated Cijs
D1=-4, D2=4
D1=-4, D2=8
D1=-4, D2=16
D1=-8, D2=4
D1=-8, D2=8
D1=-8, D2=16
D1=-16, D2=4
D1=-16, D2=8
D1=-16, D2=16
SuT-i
SuT-j

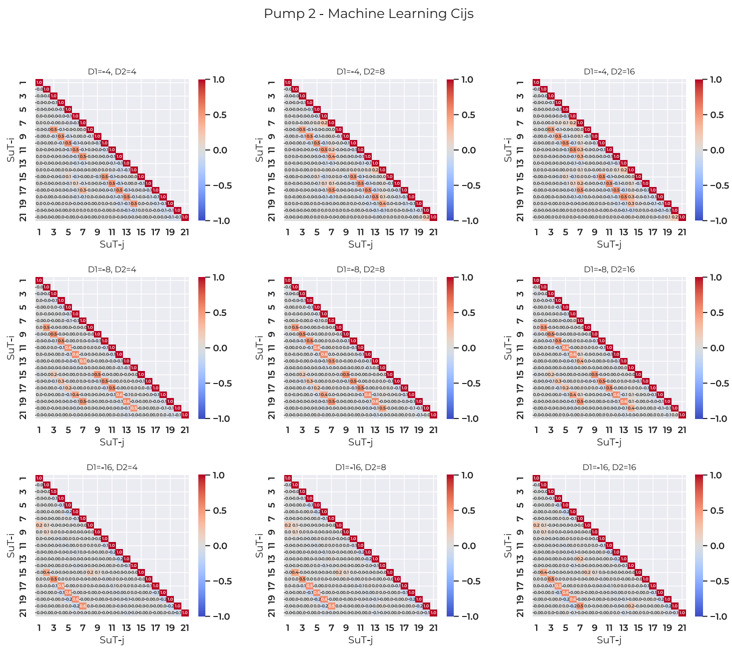
Pump 2 - Machine Learning Cijs
D1=-4, D2=4
D1=-4, D2=8
D1=-4, D2=16
D1=-8, D2=4
D1=-8, D2=8
D1=-8, D2=16
D1=-16, D2=4
D1=-16, D2=8
D1=-16, D2=16
SuT-i
SuT-j

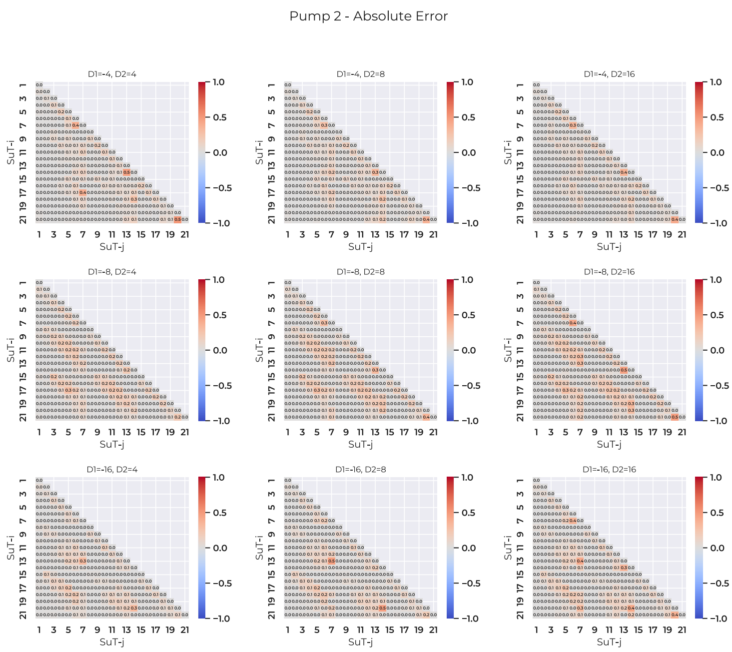
Pump 2 - Absolute Error
D1=-4, D2=4
D1=-4, D2=8
D1=-4, D2=16
D1=-8, D2=4
D1=-8, D2=8
D1=-8, D2=16
D1=-16, D2=4
D1=-16, D2=8
D1=-16, D2=16
SuT-i
SuT-j

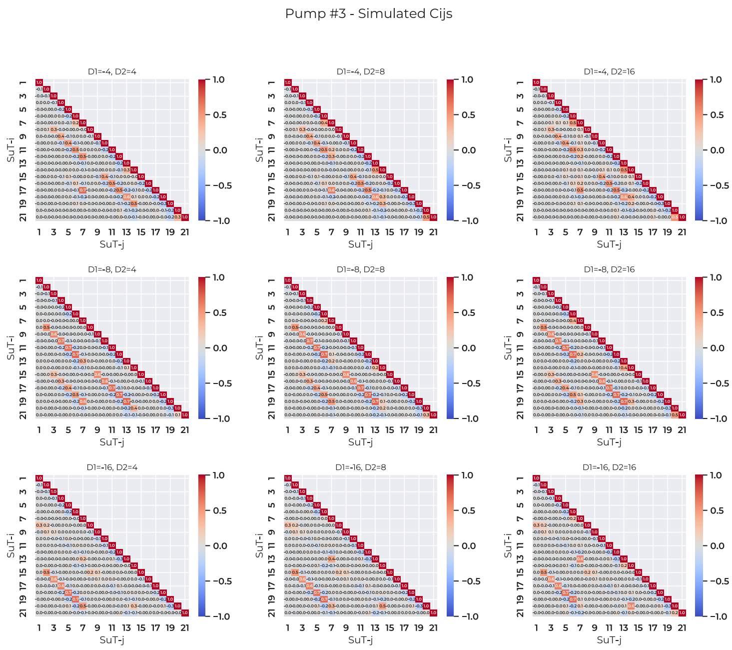
Pump #3 - Simulated Cijs
D1=-4, D2=4
D1=-4, D2=8
D1=-4, D2=16
D1=-8, D2=4
D1=-8, D2=8
D1=-8, D2=16
D1=-16, D2=4
D1=-16, D2=8
D1=-16, D2=16
SuT-i
SuT-j
1 3 5 7 9 11 13 15 17 19 21
1.0
0.5
0.0
−0.5
−1.0

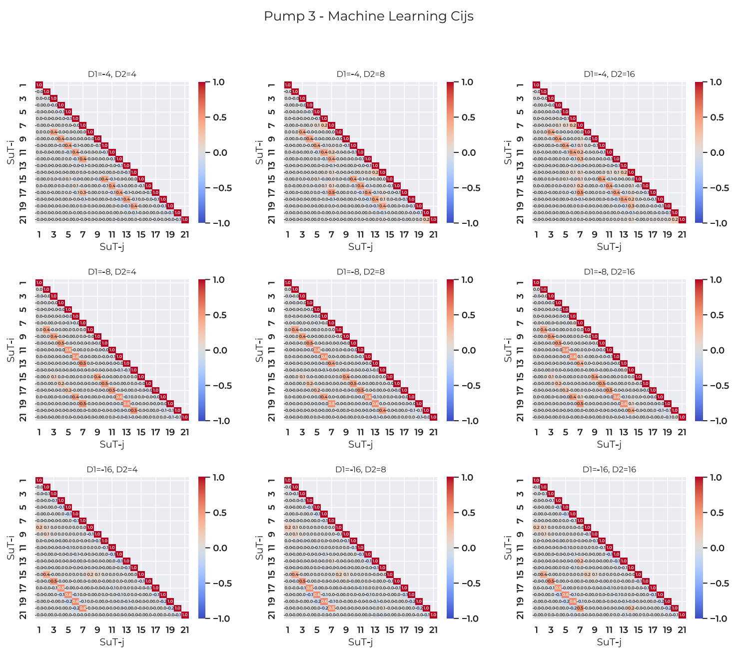
Pump 3 - Machine Learning Cijs
D1=-4, D2=4
D1=-4, D2=8
D1=-4, D2=16
D1=-8, D2=4
D1=-8, D2=8
D1=-8, D2=16
D1=-16, D2=4
D1=-16, D2=8
D1=-16, D2=16
SuT-i
SuT-j
1 3 5 7 9 11 13 15 17 19 21
1.0
0.5
0.0
−0.5
−1.0

Pump 3 - Absolute Error

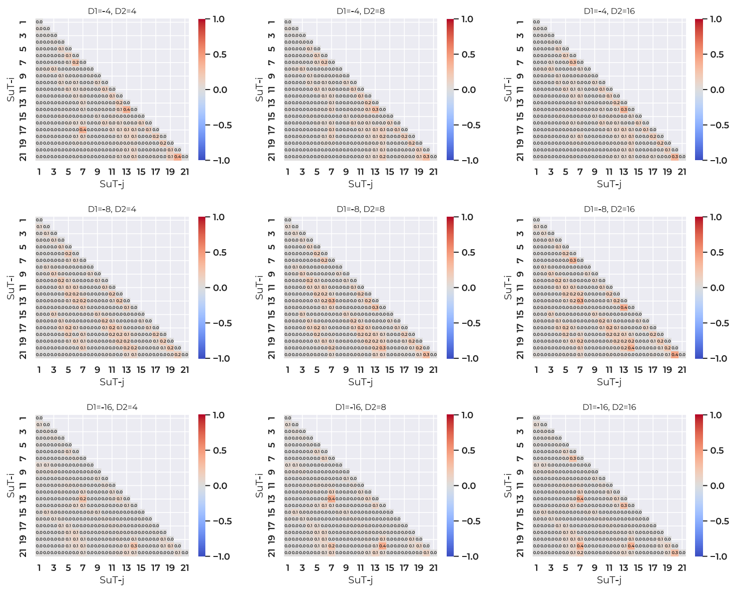

Pump #4 - Simulated Cijs

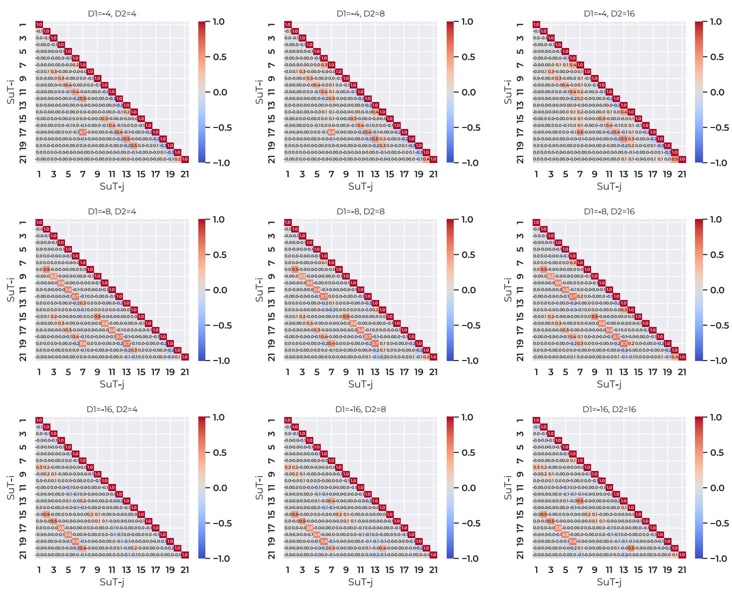

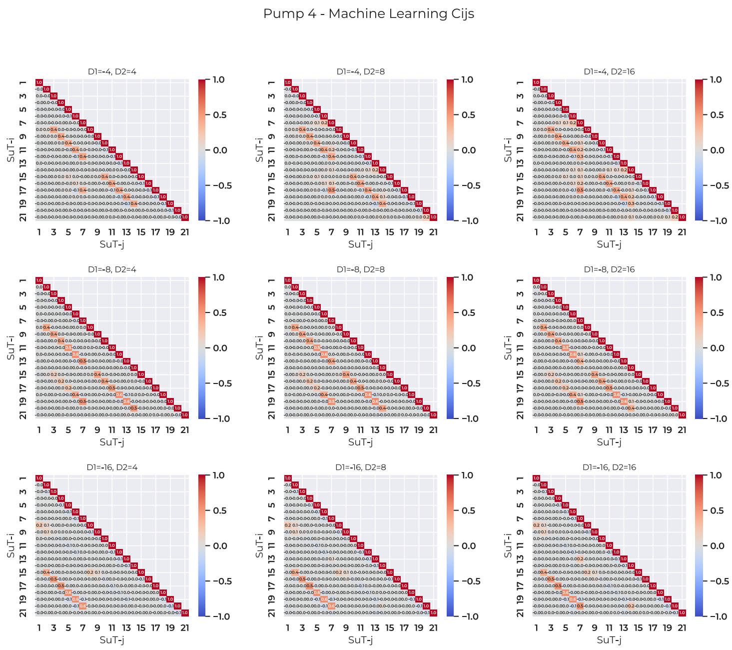

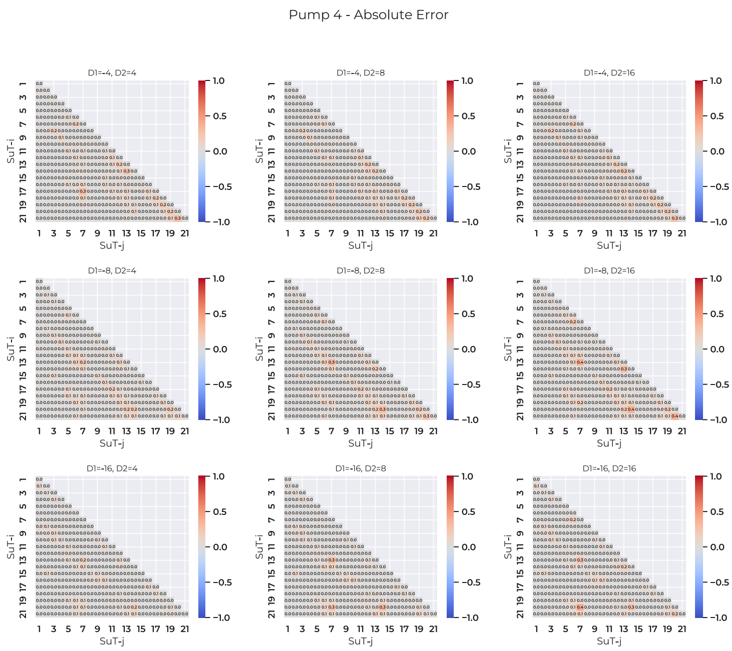

On simulated correlation coefficients there are many possible observations to make: in all the plots, we can notice subsets of cells which absolute value is way higher with respect nearby ones: we will refer to these cells as resonances. Main resonances found are diagonal ones, which are triggered by accumulated dispersion $\beta_{2,acc,(i,j)}$ approaching zero, and start to appear when row index $i > 7$, so when we have first chromatic dispersion compensation by DCF. Instead, vertical and horizontal resonances seem to appear mostly in span indexes i and j where dispersion compensation acts, but their cause is not completely clear yet. Diagonal resonances are more or less equal in scenarios with equal D_1 (regarding the same pump of course), but among variation on just D_2, vertical and horizontal resonances become more intense with increasing D_2, as it's particularly noticeable in scenarios with $D_1 = -4$. Another observation that can be done is that in XCI case, rather than SCI, we observe negative correlation coefficients in some cells: that means that such span couples decreases overall NLI figure instead of increasing it: here we find what is usually referred as "anti-coherency".

For what concerns Machine Learning predictions, as expected by looking at spatially disaggregated curves, guess very well the behavior of the actual correlation coefficients, returning a quick and accurate estimation just based on fiber and spectrum parameters.

4.3 Full Superposition: Overall NLI Estimation

Finally, we combine spatial and spectral disaggregation in the complete 9-channels scenario to estimate the entire NLI through the presented model:

- Black curve is obtained computing each span coherent contributions via equation (4.4), with GN Model normalized NLIs and Machine Learning C_{ij} for each pump, combined through equation (4.2)

- Red curve is the multichannel ground truth, already seen in Figures 4.4 and 4.5

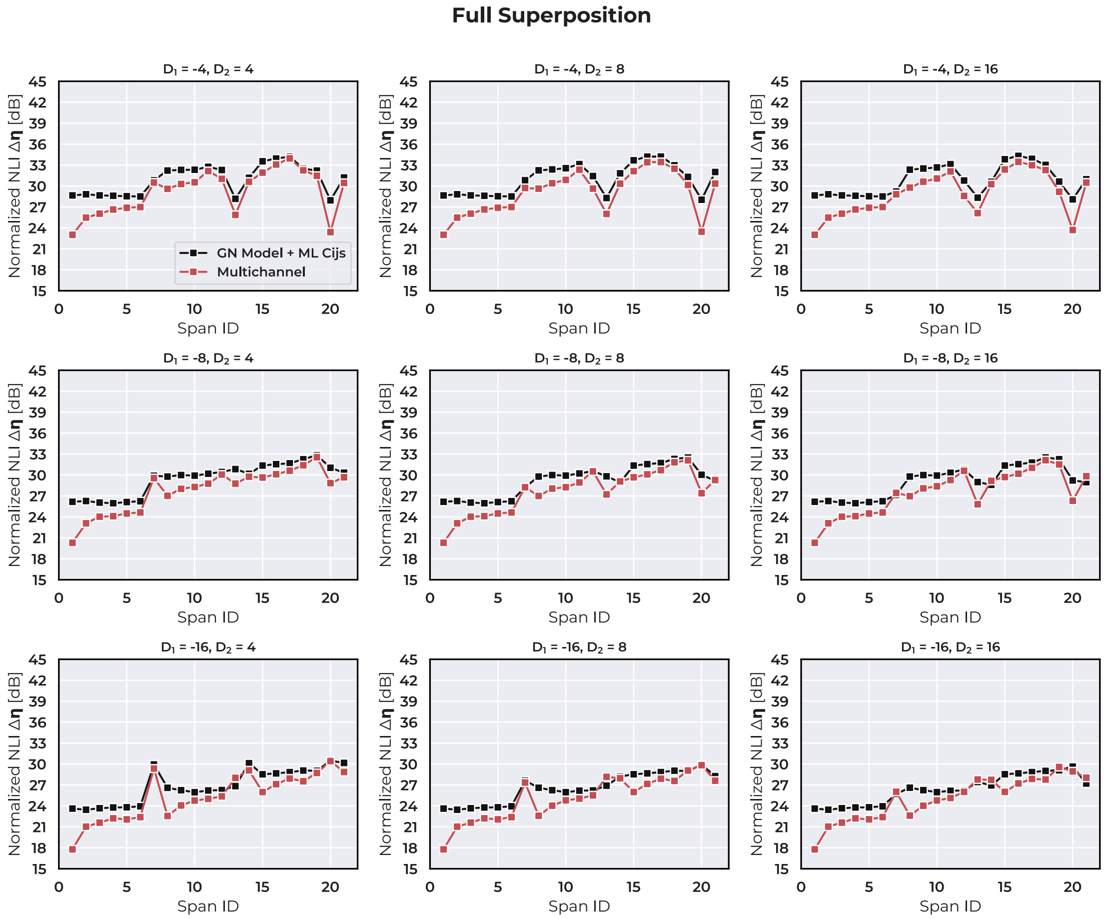
Full Superposition
D1 = -4, D2 = 4
D1 = -4, D2 = 8
D1 = -4, D2 = 16
D1 = -8, D2 = 4
D1 = -8, D2 = 8
D1 = -8, D2 = 16
D1 = -16, D2 = 4
D1 = -16, D2 = 8
D1 = -16, D2 = 16
Normalized NLI Δη [dB]
Span ID
GN Model + ML Cijs
Multichannel

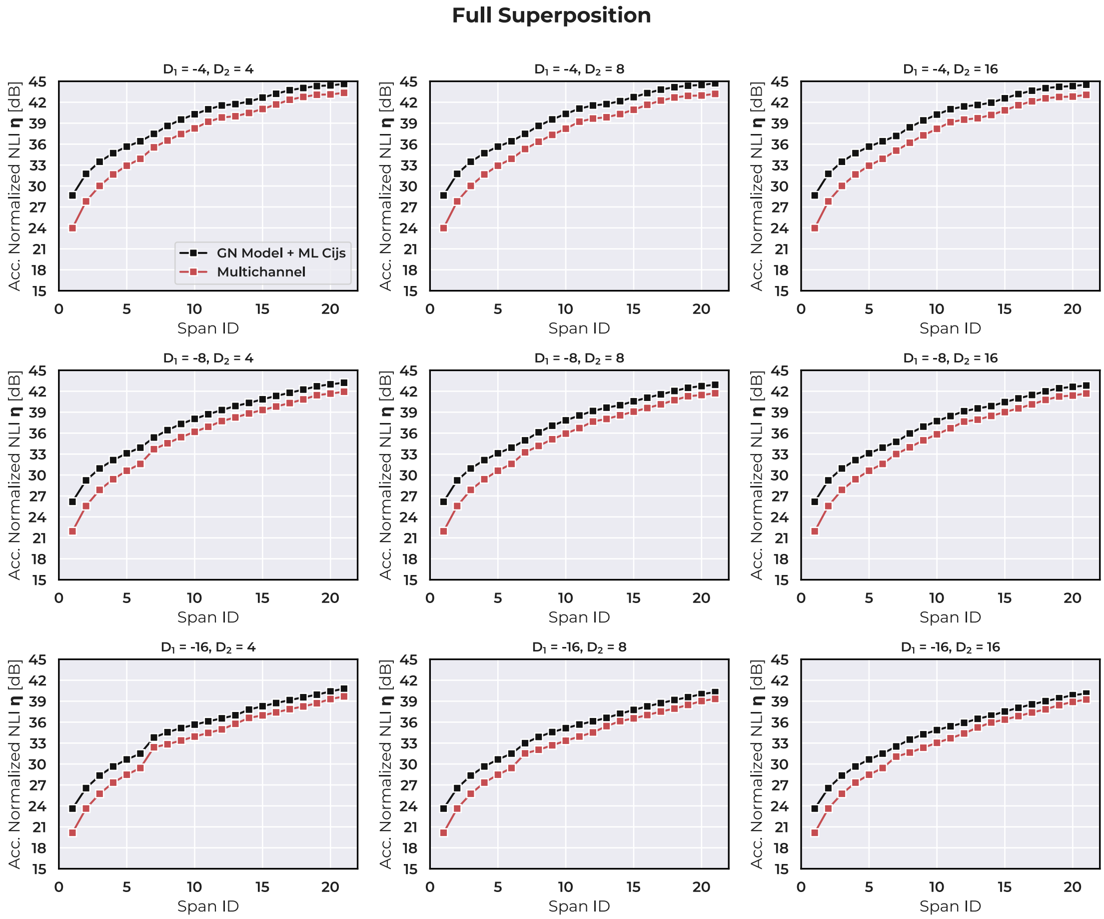

In these figures, black curve (output of presented modeling) gives a pretty accurate, conservative estimation of red one (our target). This is something expected since spectral disaggregation reconstructed almost perfectly ground truth, while spatial disaggregation reconstructed each SCI and XCI component perfectly with simulated pure contributions and correlation coefficients and with gaussianization conservativity gap for what concerns semi-analytical model output, resulting in an overall conservative evaluation, about 1-2 dB at the end of the link depending on the single scenario.

We remark that here the main gain is obtained in terms of computational resources and time: in order to obtain each red curve, simulation time required is in the order of days and moreover that computation is forced to require a GPU. Computational time required for black curve instead is in the order of milliseconds, making the process practically instantaneous, even with just CPU.

4.4 GSNR evaluation for $D_1 = -4$ and $D_2 = 16$ case

In the tested scenarios, we analyzed normalized NLI η metric behavior, being an all-encompassing NLI metric which does not depend on channels power. As seen in equations (1.29), (1.30) and (1.31), passing from η parameter to SNR_{NLI} is immediate, but final metric to use for BER evaluation is GSNR, as seen in formula (1.28), which includes also the OSNR contribution. Among the tested scenarios, the one with $D_1 = -4$ and $D_2 = 16$ is the one in which DCF span length (Table 4.2) is nearer to realistic values used in actual scenarios, and maybe it's also the most interesting one from coherency point of view since its correlation coefficients heatmaps presents the strongest already discussed vertical and horizontal resonances on compensating spans. The problem with such too high length values is that, since EDFAs operates in transparency, amplifiers gains have to completely compensate span loss and with such long fibers, losses results to be very intense bringing ASE values to explode, due to direct proportionality with Gain G (equation (1.26)), so the final resulting GSNR is so low (several tens of dB below zero) to not make any sense for an optical communication system to work in such conditions, and even just for our scopes, OSNR would completely cover SNR_{NLI} both on semi-analytical curve and simulated one, making totally non-appreciable NLI modeling. On the other hand, is useful to see at least one time the combined impact of both NLI and OSNR on final GSNR: adding same OSNR value to both red curve and black one, basically worsen the system performances, making the two curves closer, even converging to same values.

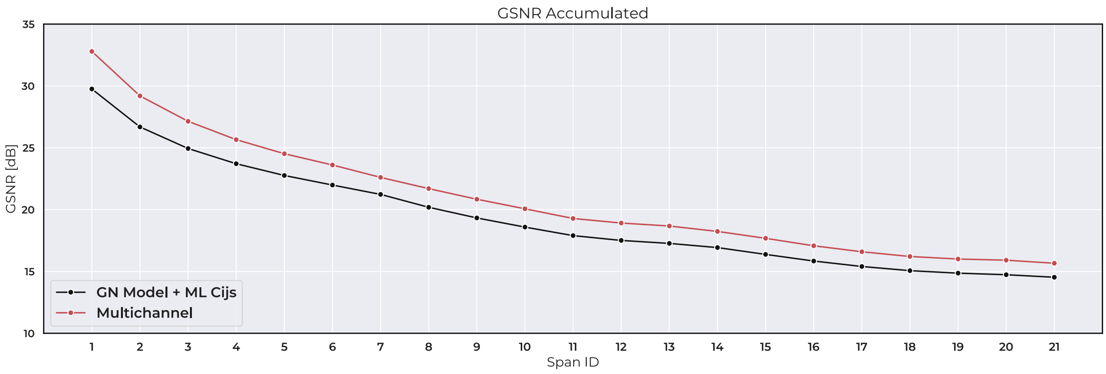

Figure 4.9: GSNR for $D_1 = -4$ and $D_2 = 16$ case

In Figure 4.9 we can see the final result, remarking the fact that, since GSNR is proportional to SNR_{NLI}, which is inversely proportional to η, GSNR is inversely proportional to η, therefore a GSNR underestimation corresponds to conservativity as seen for Normalized NLI, so that's a further confirmation of model consistency. In that case, we have around 1 dB conservativity at the end of the link.

Chapter 5

Conclusions

We started this thesis with a brief overview of actual scenarios in optical networks world, remarking the need for a quick QoT estimation tool for NLI in DM scenario. In Chapter 1 we reported the main physical phenomena (useful in that context) involved in optical signal propagation, analyzing chromatic dispersion and Kerr effect disturbances, and how they are took into account by NLSE field propagation equation. These concepts were fundamental to understand the various physical dependencies in that problem as well as main premises, ideas and conditions on which GN model relies, which we have seen to be a worst case NLI analytical estimation in UT context. As we have shown numerically in Chapter 4, GN model alone is not suited to address the NLI estimation problem in DM scenario: in Chapter 2 we abstracted a generic DM OLS system to develop a proper analytical expression to address NLI noise propagation with the presence of chromatic dispersion compensation units, and the outcome was formula (2.3), which depends only on pure NLI contributions, that are estimated with GN Model and correlation coefficients, which are predicted with Machine Learning methods through a Random Forest regressor, trained on a large dataset made of simulations data. Combining SCI and XCI contributions obtained with mentioned before formula through channels NLI superposition (spectral disaggregation), we obtained a full spectral load estimation model for each span. In order to validate that model, ground truth data for comparison were required: for that purpose, in Chapter 3 we presented the simulator on which we relied on: a Matlab-based SSFM tool, which simulates numerically signal propagation via NLSE in a customized optical link, returning main metrics of interest. Finally in Chapter 4, we validated the entire model under spatial and spectral disaggregation profiles: firstly, we shown that aggregated ground truth NLI can be very well approximated by summing up each channel non-linear contribution through spectral disaggregation approach, then we tested out spatial disaggregation formula for NLI evaluation on each span. That formula came out to predict almost perfectly NLI figure for each pump and probe configuration if input data σ_i, σ_j and C_{ij} are taken from simulations, while if we input σ_i and σ_j taken from GN Model and C_{ij} from ML predictions, the resulting semi-analytical NLI overestimates simulated one with a displacement due almost only to GN Model gaussianization, since ML predictions on correlation coefficients are pretty accurate. So putting all SCI and XCIs effect together, final full spectral load disaggregated semi-analytical estimation matches very well the aggregated simulated one, remaining as displacement just the GN Model conservativity gap mentioned before. Although is good to have a worst case estimation, on the other hand this gap make the system not exploitable at the maximum of its possibilities: approaches to account for gaussianization have been proposed in aggregated scenario like as EGN [4], but literature lacks of such solution in disaggregated scenario, which can be the object for future works investigations, as well as an analytical approach to correlation coefficients estimation.

Appendix A

Proof of Coherency Power Expression

We have to develop the term

$$\mathbb{E}\left[n_k n_i^* \prod_{j=k}^{i-1} d_j + n_k^* n_i \prod_{j=k}^{i-1} d_j^*\right] \tag{1}$$

That we can write as

$$\mathbb{E}[n_k n_i^*] \prod_{j=k}^{i-1} d_j + \mathbb{E}[n_k^* n_i] \prod_{j=k}^{i-1} d_j^* \tag{2}$$

Since dispersion terms have no statistical dependence. In general, given two random processes X and Y, it holds:

$$\mathbb{E}[XY^*] = \mathbb{E}[X^*Y]^* \tag{3}$$

So, in our case, expression (2) become:

$$\left(\mathbb{E}[n_k^* n_i] \prod_{j=k}^{i-1} d_j^*\right)^* + \mathbb{E}[n_k^* n_i] \prod_{j=k}^{i-1} d_j^* \tag{4}$$

Using complex numbers properties, this results to be:

$$2\Re\left(\mathbb{E}[n_i n_k^*] \prod_{j=k}^{i-1} d_j^*\right) \tag{5}$$

$$2\mathbb{E}\left[\Re\left(n_i n_k^* \prod_{j=k}^{i-1} d_j^*\right)\right] \tag{6}$$

That is the expression we were looking for.

Bibliography

[1] Govind P Agrawal and AE Willner. «Fiber-Optic Communication System». In: *IEEE Journal of Quantum Electronics-Institute Electrical and Electronic Engineers* 30.2 (1994), pp. 347–347 (cit. on p. 1).

[2] Pierluigi Poggiolini, Gabriella Bosco, Andrea Carena, Vittorio Curri, Yanchao Jiang, and Fabrizio Forghieri. *A Detailed Analytical Derivation of the GN Model of Non-Linear Interference in Coherent Optical Transmission Systems.* 2012. URL: `https://arxiv.org/pdf/1209.0394` (cit. on p. 6).

[3] Emanuele Virgillito, Andrea Castoldi, Andrea D'Amico, Stefano Straullu, Andrea Bovio, Rosanna Pastorelli, and Vittorio Curri. «Spatially disaggregated model for self-channel interference in mixed fiber optical network segments». In: *Journal of Optical Communications and Networking* 15.8 (2023), pp. C271–C287. DOI: `10.1364/JOCN.486713` (cit. on p. 16).

[4] Andrea Carena, Gabriella Bosco, Vittorio Curri, Yanchao Jiang, Pierluigi Poggiolini, and Fabrizio Forghieri. «EGN model of non-linear fiber propagation». In: *Optics express* 22.13 (2014), pp. 16335–16362 (cit. on p. 58).